SWI/SNF antagonizes SIR heterochromatin to promote transcription of genes expressed during mitotic exit in *Saccharomyces cerevisiae*

Mayuri Rege[1,2], Jessica L. Feldman[1], Nicholas L. Adkins[1], and Craig L. Peterson[1,3]

[1] Program in Molecular Medicine, University of Massachusetts Medical School

373 Plantation Street, Biotech 2, Suite 210, Worcester, MA 01605

[2]Current Address: DST-INSPIRE faculty, Department of Microbiology, Ramnarain Ruia Autonomous College, Matunga, Mumbai- 400019, India

[3]Corresponding author

19 Running Title: SWI/SNF antagonizes SIR heterochromatin

20

21 Key Words: SWI/SNF, heterochromatin, transcription, pseudo-diploid, SIR, INO80, HST

22

23 Corresponding author:

24 Craig L. Peterson

25 373 Plantation Street, Biotech 2, Suite 210, Worcester, MA 01605

26 Email: craig.peterson@umassmed.edu; Ph#508-856-5858

27

ABSTRACT:

Heterochromatin is a repressive, specialized chromatin structure that is central to eukaryotic transcriptional regulation and genome stability. In the budding yeast, *Saccharomyces cerevisiae*, heterochromatin formation requires Sir2p, Sir3p, and Sir4p, and these Sir proteins create specialized chromatin structures at telomeres and silent mating type loci. Previously, we reported that the SWI/SNF chromatin remodeling enzyme can evict Sir3 from chromatin fibers *in vitro*, though whether this activity contributes to the role of SWI/SNF as a transcriptional activator at euchromatic loci is unknown. Here, we characterize genetic interactions between the *SIR* genes (*SIR2*, *SIR3*, and *SIR4*) and genes encoding subunits of the chromatin remodelers SWI/SNF and INO80C, as well genes encoding the histone deacetylases Hst3 and Hst4. We find that loss of *SIR* genes partially rescues the growth defects of *swi2*, *ino80*, and *hst3/hst4* mutants during replication stress conditions. Interestingly, partial suppression of *swi2*, *ino80*, and *hst3 hst4* mutant phenotypes is due to the pseudo-diploid state of *sir* mutants, but a significant portion is due to more direct functional interactions. Consistent with this view, transcriptional profiling of strains lacking Swi2 or Sir3 identifies a set of genes whose expression in the M/G1 phase of the cell cycle requires SWI/SNF to antagonize the repressive impact of Sir3.

INTRODUCTION

Eukaryotic genomes are packaged with positively charged histone proteins to form chromatin. Chromatin can be divided into two functional categories: transcriptionally active euchromatin and transcriptionally silent heterochromatin. In budding yeast, heterochromatic structures are formed at each telomere and the two silent mating type loci (*HMR* and *HML*). The assembly of heterochromatin domains requires the binding of non-histone proteins to the chromatin fiber, and in yeast these are Sir2, Sir3 and Sir4 (Rusche *et al.* 2003; Rusché *et al.* 2002). Sir3 is believed to be the structural component of yeast heterochromatin, whereas Sir2 is a histone deacetylase that functions with Sir4 to target Sir proteins to the proper genomic locations. Deletion of *SIR* genes leads to expression of both a- and α-specific genes in haploids, producing a pseudo-diploid state (Haber 1998). Previous studies have found that this pseudo-diploid state alters the DNA damage response, alleviating the genotoxic stress phenotypes of several *rad* mutants (Schild 1995; Valencia-Burton *et al.* 2006).

In addition to heterochromatic regions, Sir3 has also been detected by chromatin immunoprecipitation studies at euchromatic locations, although the functional implications are not understood (Radman-Livaja *et al.* 2011). Immunofluorescence studies of Sir3 have also revealed that Sir3 forms discrete nuclear puncta for most of the cell cycle, except for a diffuse nuclear staining pattern during mitotic stages (Laroche *et al.* 2000). Overexpression of Sir3 can lead to the expansion of heterochromatin domains and gene-silencing defects within euchromatin (Taddei *et al.* 2009; Holmes *et al.* 1997), indicating that aberrant binding of Sir3 to euchromatic sites can be detrimental.

ATP-dependent chromatin remodeling enzymes are a major contributor to the dynamic nature of chromatin. They modify chromatin structure by mobilizing or disrupting nucleosomes in

an ATP-dependent reaction (Clapier and Cairns 2009). The SWI/SNF chromatin remodeling enzyme is a founding member of this group of enzymes (Smith and Peterson 2005), and subunits of SWI/SNF were first identified in yeast genetic studies as global activators of transcription (Peterson *et al.* 1992; Laurent *et al.* 1991). For instance, inactivation of the Swi2 ATPase subunit leads to defects in the transcription of many inducible yeast genes, as well the function of many transcriptional activators. Strains harboring mutations in genes encoding SWI/SNF subunits have severe growth defects, are sensitive to DNA damaging or replication stress agents, and show a defect in mitotic exit (Krebs *et al.* 2000). Similar to other remodeling enzymes, SWI/SNF can use the energy of ATP hydrolysis to mobilize nucleosomes in cis, or evict nucleosomal H2A/H2B dimers as well as entire histone octamers from DNA. Recently, we also found that SWI/SNF has the novel ability to catalyze the displacement of the Sir3 protein from nucleosomal substrates *in vitro*. This activity is not shared with other remodeling enzymes, and it requires a direct interaction between the Swi2 subunit and Sir3. This activity appears to be important for cells to contend with replication stress (Manning and Peterson 2014).

In this work, we report genetic interactions between the gene encoding the Swi2 subunit of SWI/SNF and genes encoding the Sir2, Sir3, and Sir4 heterochromatin components. Inactivation of Sir3 alleviated the slow growth phenotype of a *swi2*Δ strain, and partially restored resistance to the replication stress agent, hydroxyurea (HU). Deletion of *SIR2* or *SIR3* also partially suppressed the replication stress phenotypes caused by loss of the INO80C chromatin remodeling complex as well as the loss of the H3 lysine 56-specific histone deacetylases Hst3 and Hst4. Interestingly, in some cases partial suppression of genotoxic stress phenotypes were observed in pseudo-diploid cells, suggesting indirect as well as direct impacts of Sir3 loss. To identify potential transcriptional targets for the SWI/SNF-Sir3 antagonism, we characterized the transcriptional profile of *swi2*Δ,

*sir3*Δ, and *swi2*Δ *sir3*Δ strains. A parallel analysis was also performed in *SIR3* and *sir3*Δ strains where Swi2 was conditionally depleted from the nucleus by the anchor away method (Haruki *et al.* 2008). This latter method circumvented transcriptional defects due to the severe growth phenotype of the *swi2*Δ strain, and together identified a common set of genes where SWI/SNF promotes transcription by antagonizing Sir3.

MATERIALS AND METHODS:

Yeast growth media and genetic methods

Yeast were cultured using standard procedures (Rege *et al.* 2015). For tetrad analysis, at least 30 tetrads were dissected for segregation analysis and growth rates noted.

List of strains

Name	***Genotype***
CY1653	*BY4743; MATa/a ;his3Δ1/his3Δ1; leu2Δ0/leu2Δ0; lys2Δ0/LYS2; MET15/me ura3Δ0/ura3Δ0; swi2::KanMX4/SWI2 sir3Δ:: HPH^R/SIR3*
CY1618	*MAT (a) segregant from CY1653, clone 15A, sir3Δ::HPH*
CY1619	*MAT (a) segregant from CY1653, clone 15B, swi2Δ::KANMX and sir3Δ::HP*
CY1620	*MAT a segregant from CY1653, clone 15C (wild type)*
CY1621	*MAT a segregant from CY1653, clone 15D, swi2::KANMX*
CY1809	*Y40345 MATa tor1-1 fpr1::loxP-LEU2-loxP RPL13A-2x FKBP12:loxP (HH*
CY1810	*Y40362 MATα tor1-1 fpr1::NAT RPL 13A-2x FKB12::TRP1 SNF2-FRB:kan*
CY1853	*MAT a sir3Δ::HYGRO^R in CY1809, clone 1*
CY1854	*MAT α, sir3Δ::HYGRO^R in CY1810, clone 16*
CY1953	*MATα sir2Δ::HIS in CY1885, clone 12*

CY1954	*MATα sir2Δ::HIS in CY1810, clone 10*
CY1907	*MATa/a ;his3Δ1/his3Δ1; leu2Δ0/leu2Δ0; lys2Δ0/LYS2; MET15/met15Δ0; ura3Δ0/ura3Δ0; swi2::KanMX4/SWI2 sir2Δ:: HPH^R/SIR2*
CY1908	*MATa/a ;his3Δ1/his3Δ1; leu2Δ0/leu2Δ0; lys2Δ0/LYS2; MET15/met15Δ0; ura3Δ0/ura3Δ0; swi2::KanMX4/SWI2 sir4Δ:: HPH^R/SIR4*
CY1752	*MATa/α CY927 X CY971; sir3Δ::HYGRO^R, diploid 2*
CY2041	*swi2Δ in W303, spore 21A dissected from CY1752*
CY2042	*sir3Δ in W303, spore 21B dissected from CY1752*
CY2043	*WT in W303, spore 21C dissected from CY1752*
CY2044	*swi2Δ sir3Δ in W303, spore 21D dissected from CY1752*
CY2394	*Y40345 MATa tor1-1 fpr1::loxP-LEU2-loxP RPL13A-2×FKBP12::loxP (H bar1Δ::HISG RPB3-FLAG:NAT*
CY2395	*Y40345 MATa tor1-1 fpr1::loxP-LEU2-loxP RPL13A-2×FKBP12::loxP (H bar1Δ::HISG HST3-FRB:kanMX6 hst4Δ::HPH RPB3-FLAG:NAT*
CY1838	*Y40345 MATa tor1-1 fpr1::loxP-LEU2-loxP RPL13A-2×FKBP12::loxP (H bar1Δ::HISG INO80-FRB:His3MX6*
CY2478	*MATa sir3Δ::PHL in CY2395*
CY2479	*MATa sir2Δ::PHL in CY2395*
CY2186	*MATa sir2Δ::KanMX in CY1838*
CY2162	*MATa sir3Δ::KanMX in CY1838*
CY2190	*MATa sir4Δ::KanMX in CY1838*
CY2254	*ino80::KanMX sir3::Hygro^R clone 1D, segregant from CY 2249*
CY2252	*ino80::KanMX clone 1B, segregant from CY2249*
CY2487	*MATα nej1Δ::PHL in CY1810*
CY2488	*MATα rme1Δ::PHL in CY1810*
CY2491	*MATα pst2Δ::PHL in CY1810*
CY2485	*MATa nej1Δ::PHL in CY2395*
CY2486	*MATa rme1Δ::PHL in CY2395*

CY2492	*MATa pst2Δ::PHL in CY2395*
CY2495	*MATa nej1Δ::PHL in CY1838*
CY2496	*MATa rme1Δ::PHL in CY1838*
CY2490	*MATa pst2Δ::PHL in CY1838*
CY2495	*MATa nej1Δ::PHL in CY1809*
CY2496	*MATa rme1Δ::PHL in CY1809*
CY2489	*MATa pst2Δ::PHL in CY2394*

Plasmid	
CP1212	pAG25; CEN/ARS w/ NAT cassette. Plasmid #35121 (Addgene)
CP1234	CEN/ARS SIR3 w/ NAT cassette
CP1	YCp50; CEN/ARS w/ URA3 cassette
CP1241	pJR156 CEN/ARS *MATa* in YCp50 w/ URA3 cassette (Jasper Rine)
CP1242	pJR157s CEN/ARS *MATα* in YCp50 w/ URA3 cassette (Jasper Rine)

Chromatin Immunoprecipitation (ChIP)

Yeast strains were grown in rich media with 2% glucose at 30°C and either DMSO or Rapamycin (8μg/ml final concentration) was added for 60 minutes before fixation with 1.2% formaldehyde. Cells were quenched with 2.5M glycine, centrifuged, rinsed with cold water and stored at -80°C until chromatin preparation. Chromatin preparation, immunoprecipitation and DNA extraction were performed as described in (Bennett *et al.* 2013). The anti-Sir3 antibody (1 μL for 100μL chromatin) was used to immunoprecipitate native Sir3. The anti-H3 antibody, ab1791 from Abcam (1 μL for 100μL chromatin) was used to immunoprecipitate histone H3. The *SIR3* gene was C-terminally tagged with a FLAG tag and an anti-FLAG antibody used for immunoprecipitation.

Microarray sample preparation and analysis:

Yeast strains were grown in rich media with 2% glucose at 30°C in 50 ml cultures, collected at OD = 0.8 for RNA preparation and RNA was extracted using the hot phenol method as described previously (Rege *et al.* 2015). Samples prepared as described in Welch *et al.* 2007 were hybridized to Affymetrix Yeast 2.0 arrays from four replicates of *swi2*Δ and *swi2*Δ *sir3*Δ strains and analyzed by limma analysis in R (Bioconductor package). Yeast strains were grown in rich media with 2% glucose at 30°C to OD = 0.6. and either DMSO or Rapamycin (8µg/ml final concentration) was added for 60 minutes and pelleted for RNA preparation (Rege *et al.* 2015). One replicate each of the *SWI2-FRB*, *SWI2-FRB sir3Δ* and *sir3Δ* arrays and corresponding WT arrays was used. Total RNA was hybridized on Affymetrix Yeast 2.0 arrays and analyzed using a log2 fold change cut-off. The raw data files have been deposited on the GEO database (# in process).

qRT-PCR

Samples for total RNA were prepared and qRT-PCR was performed as described previously in Manning and Peterson 2014.

Data Availability Statement

All strains made in this study are available upon request from the Peterson lab. The lists of Group 1_KO genes and Group 1_AA genes are given in Table S1 and Table S2, respectively. The list of Group 1 genes common in the KO and AA datasets are given in Table S3. The lists of Group 2_KO genes and Group 2_AA genes are given in Table S4 and Table S5, respectively. RMA normalized data obtained using GeneSpring Affymetrix Software for all the conditions and replicates are

provided in Tables S5 and S6. Raw microarray .CEL files have been deposited in NCBI's GEO database with the accession number (in process).

RESULTS:

The slow growth phenotype of *swi2*Δ is partially rescued by *sir3*Δ

An isogenic set of wildtype, *sir3*Δ, *swi2*Δ, and *swi2*Δ *sir3*Δ strains was created by tetrad dissection from a swi2Δ/*SWI2 sir3*Δ/*SIR3* heterozygous diploid. Deletion of *SIR3* partially suppresses the growth defect of *swi2*Δ on rich media (Figure 1A), suggesting that these loci genetically interact. Importantly, this suppression segregates with markers for the double mutant after tetrad analysis, eliminating the possibility that a nonspecific, background suppressor causes the growth suppression in *swi2*Δ *sir3*Δ strains (Figure 1A). We also find that the growth defects of *swi2*Δ are suppressed by *sir3*Δ in a different strain background (w303; Figure 1B). In addition to slow growth on glucose media, *swi2*Δ mutants are unable to metabolize alternative carbon sources like raffinose, galactose, glycerol, or ethanol (Abrams *et al.* 1986; Carlson *et al.* 1981). Inactivation of Sir3 did not facilitate growth of a *swi2*Δ on raffinose, but limited suppression was observed for growth on media containing galactose, ethanol, or glycerol (Figure 1C). *SWI2* is also required for resistance to replication stress, induced by hydroxyurea (HU), and a *swi2*Δ shows a delayed growth rate in this condition (Sharma *et al.* 2003). Interestingly, deletion of *SIR3* partially relieves the HU sensitive phenotype of a *swi2*Δ (Figure 1C). Thus, a subset of *swi2*Δ phenotypes are alleviated by deletion of *SIR3*.

To completely eliminate the possibility that a background mutation other than the *sir3*Δ segregated with, and caused the growth suppression seen in the double mutant, we transformed the *swi2*Δ *sir3*Δ with a plasmid containing *SIR3* expressed from its endogenous promoter. As

161 expected, complementation with a vector plasmid had no impact on growth, while the *SIR3*
162 plasmid slowed the growth of the *swi2*Δ *sir3*Δ strain (Figure 1D). Given that *sir3*Δ suppresses the
163 severe growth defects of *swi2*Δ in multiple strain backgrounds, and that this suppression can be
164 reversed when *swi2*Δ *sir3*Δ is complemented by a *SIR3* plasmid, these data suggest that SWI/SNF
165 antagonizes Sir3 *in vivo*.
166
167 **Absence of *SIR2* does not suppress *swi2*Δ growth defects**
168 Given that *SIR3* shows negative genetic interactions with *SWI2*, we asked whether genes that
169 encode other Sir proteins, Sir2 and Sir4, also showed similar genetic interactions. Sir2 is a histone
170 deacetylase (HDAC) that promotes Sir3 binding to nucleosomes by removing the acetyl group on
171 histone H4 lysine 16. Sir4 forms a complex with Sir2, and it is believed to play a key role in
172 targeting Sir proteins to telomeres and HM loci (Rusché *et al.* 2002; Thurtle and Rine 2014).
173 Unlike deletion of *SIR3*, inactivation of Sir2 did not alleviate the slow growth of the *swi2*Δ (Figure
174 S1A, B). In contrast, inactivation of Sir4 suppresses the growth defect of a *swi2*Δ mutant (Figure
175 S1C, D). Thus, the studies support genetic interactions between *SWI2*, *SIR3*, and *SIR4*, but not
176 *SIR2*.
177
178 **Comparison of *swi2*Δ alleles with conditional depletion of Swi2**
179 As *swi2*Δ null mutants are extremely slow growing, we wanted to establish an alternative approach
180 to interrogate the genetic interactions between *SIR* genes and *SWI2*. To this end, the anchor away
181 system was used to conditionally deplete Swi2 from the nucleus (Haruki *et al.* 2008). The parent
182 strain harbors a FK506 binding protein (FKBP12) tag fused to the C-terminus of an anchor protein,
183 RPL13A. RPL13A is a ribosomal protein that is present in high copy numbers in the cell and

184 transits from the nucleus to the cytoplasm during ribosome assembly, as shown in Figure 2A. In
185 this parent strain, we tagged the endogenous *SWI2* locus at the C-terminus with the FKBP12-
186 rapamycin-binding (FRB) domain. Rapamycin induces formation of a ternary complex between
187 the FKBP12 and FRB domains, and thus, rapidly depletes *SWI2*-FRB from the nucleus (Figure
188 2A).

189 We first compared growth rates of *SWI2*-FRB strains with or without the *SIR3* gene using
190 spot assays. In the presence of DMSO solvent, growth rates of all strains are identical on rich
191 media (Figure 2B), indicating that the *SWI2-FRB* fusion itself does not impair Swi2 function. In
192 the presence of rapamycin, *SWI2-FRB* strains show a decrease in growth rate compared to the WT,
193 consistent with nuclear depletion of Swi2 (Figure 2B). However, the *SWI2-FRB* strains have a
194 milder growth defect compared to the *swi2*Δ (null) mutant (Figure 1), perhaps due to residual Swi2
195 present in the nucleus. Similar to the *swi2*Δ, depletion of *SWI2* also causes HU sensitivity, and this
196 phenotype is partially suppressed by deletion of *SIR3*, suggesting an important link between Swi2
197 and Sir3 during replication stress (Figure 2B). Unlike the case with a deletion allele of *SWI2*,
198 deletion of *SIR2* also partially suppressed the sensitivity of the SWI2-FRB strain (+Rap) to HU,
199 but to a lesser extent than deletion of *SIR3* (Figure 2B).

200 Previous work has shown that *SWI2* is required for transcriptional activation of the
201 ribonucleotide reductase (RNR) genes in the presence of HU (Sharma *et al.* 2003). Consistent with
202 this, we see a large reduction of these transcripts in the *swi2*Δ (Figure S1E, F). However, unlike the
203 rescue of growth, the lower levels of RNR transcripts was not restored by the *sir3*Δ following
204 depletion of Swi2. This observation suggests that in HU stress, SWI/SNF may antagonize Sir3
205 independent of transcription, possibly by assisting replication within SIR heterochromatin.
206

Deletion of *SIR2* or *SIR3* suppresses growth defects of *ino80* and *hst3/hst4* mutants

To investigate whether the suppression of growth defects by loss of Sir proteins is unique to SWI/SNF or a more common feature among chromatin modifying enzymes, we determined if deletion of *SIR2* and *SIR3* suppresses the growth defects caused by nuclear depletion of the histone H3 deacetylases, Hst3 and Hst4 (*Hst4*Δ*/HST3-FRB*), or the chromatin remodeler, INO80C (*INO80-FRB*). In the presence of rapamycin, both the *Hst4*Δ*/HST3-FRB* and *INO80-FRB* strains grow similarly to WT, but they are sensitive to stress conditions, such as when media contains camptothecin (CPT) or HU (Figure 2C, D). Strikingly, deletion of either *SIR2* or *SIR3* suppresses the growth defects caused by rapamycin-dependent depletion of either Ino80 or Hst3/Hst4 in the presence of HU or CPT (Figure 2C, D). Similarly, deletion of *SIR3* also partially suppresses an *ino80*Δ strain (Figure S2), confirming the results observed with INO80 anchor away. Thus, in addition to *SWI2*, the *SIR* genes also show genetic interactions with *HST3/HST4*, and *INO80*.

Genotoxic stress is partially suppressed by *MAT* heterozygosity

Our genetic studies suggest that SWI/SNF, INO80C, and Hst3/Hst4 antagonize Sir proteins during replication stress. SIR heterochromatin prevents expression of the silent mating type loci, and consequently, loss of Sir proteins leads to expression of diploid-specific genes and suppression of haploid-specific genes (Rine and Herskowitz 1987; Goutte and Johnson 1988; Herskowitz 1989; Dranginis 1990). This pseudo-diploid state, in which both the MATa and MATα genes are expressed, is termed the *MAT* heterozygotic state. *MAT* heterozygosity has been shown to suppress the DNA repair defects of *rad* mutants (Valencia-Burton *et al.* 2006). Indeed, both MAT heterozygosity and *sir* mutants downregulate NHEJ and preferentially use HR for DNA repair (Valencia-Burton *et al.* 2006). To determine whether loss of Sir proteins suppresses replication

stress phenotypes in a direct manner or an indirect manner due to pseudo-diploid effects, we investigated the impact of *MAT* heterozygosity. We introduced an episomal copy of *MATα* into the *MAT***a** anchor away strains to generate *MATa*/*MAT*α haploids. Interestingly, MAT heterozygosity partially suppressed the sensitivity of *SWI2-FRB* (+ Rap) during HU stress (Figure 3A), though the suppression was less than what was observed by deletion of *SIR3* (Figure 2B). In contrast, MAT heterozygosity did not suppress sensitivity of SWI2-FRB (+Rap) to CPT (Figure 3A). The sensitivity of the *hst4*Δ*/HST3-FRB* and *INO80-FRB* mutants to CPT, and to a lesser extent HU, was also partially suppressed by MAT heterozygosity (Figure 3B, C). Taken together, the results indicate that the replication stress sensitivity of strains depleted for Swi2, Ino80, or Hst3/Hst4 can be partially suppressed by *MAT* heterozygosity, either by deletion of *SIR* genes or by expressing the opposite mating type in haploid strains. However, the extent of suppression by the pseudo-diploid state is generally less than what is observed for loss of Sir proteins.

Expression of both MAT**a** and MATα alters the transcriptional profile by down regulating haploid-specific genes and upregulating diploid-specific genes (Herskowitz 1989). Thus, we sought to investigate which of these pathways are important for suppressing replication stress phenotypes. Previous work has shown that deletion of the haploid-specific gene *NEJ1*, required for non-homologous end joining (NHEJ), suppressed the growth defect of *rad55*Δ when exposed to DNA damage (Valencia-Burton *et al.* 2006). To determine whether loss of NHEJ also suppresses the phenotypes due to loss of chromatin modifiers, we deleted *NEJ1* in the anchor away strains. Deletion of *NEJ1* did not suppress the growth defects of *SNF2-FRB*, *hst4*Δ*/HST3-FRB*, or *INO80-FRB* mutants when grown on rapamycin in the presence of HU or CPT (Figure S3A). We next tested the impact of two additional haploid-specific genes, *RME1* or *PST2*, which show genetic interactions with *RAD55* and *RAD51* during growth on CPT stress (Valencia-Burton *et al.* 2006).

253 However, deletion of either *RME1* or *PST2* did not suppress the HU or CPT stress phenotypes of
254 the *SWI2-FRB*, *hst4*Δ*/HST3-FRB*, or *INO80-FRB* (+Rap; Figure S3B, C). Thus, the underlying
255 genetic basis for the *MAT*-dependent, partial suppression of stress phenotypes due to depletion of
256 SWI/SNF, INO80, and Hst3/Hst4 remains unknown, though it does not appear to be due to loss of
257 NHEJ or activation of meiotic transcriptional programs.
258
259 **Loss of Sir3 partially suppresses the transcriptional defects due to loss of SWI/SNF**
260 Since loss of Sir3 has a large impact on phenotypes due to loss of Swi2 than *MAT* heterozygosity,
261 we entertained the possibility that SWI/SNF may directly antagonize transcriptional repression by
262 Sir3 at a subset of genes. To identify such transcriptional targets, we analyzed RNA profiles of
263 isogenic wild type, *swi2*Δ, *sir3*Δ, and *swi2*Δ *sir3*Δ strains for 5716 ORFs using DNA microarrays.
264 Consistent with published data, we observed that deletion of *SIR3* mis-regulates genes in the
265 mating type cascade, with almost no other changes (Figure 4A *middle*) (Lenstra *et al.* 2011). In
266 contrast, *SWI2* regulates 203 genes positively (FDR < 0.1 and LFC < -0.58) and 488 genes
267 negatively (FDR < 0.1 and LFC > 0.58) (Figure 4A *top*). Many genes whose expression is known
268 to be dependent on SWI/SNF, such as *SER3*, *YOR222W*, and the acid phosphatase genes, were
269 altered as predicted (Figure 4B) (Sudarsanam *et al.* 2000). However, these SWI/SNF-dependent
270 genes were unaffected by a deletion of *SIR3* (Figure 4B, third column).
271 To identify genes that are regulated by both *SWI2* and *SIR3*, we first selected genes that
272 changed significantly in the *swi2*Δ compared to wild type (Figure 4B), and we then performed
273 hierarchical clustering and classified various sub-groups of interest. Genes that decrease
274 significantly (LFC < -0.58 and FDR < 0.1) in *swi2*Δ and are restored to nearly wild type levels in
275 the *swi2*Δ *sir3*Δ are defined as Group 1_KO (Table S1). The top gene ontology (GO) term

category enriched in Group 1_KO is ribosome biogenesis/ ribosomal protein coding genes. This suggests that these genes require SWI/SNF to antagonize Sir3 to promote transcription. Indeed, prior studies have reported Sir3 binding to many ribosomal protein genes, using a *GAL-SIR3* inducible strain (Radman-Livaja *et al.* 2011). However, mRNA abundance of genes involved in ribosome biogenesis/ ribosomal proteins strongly anti-correlates with cellular growth rate and may confound our results (Airoldi *et al.* 2009).

To circumvent potential issues due to growth defects, we also analyzed RNA profiles from the anchor away strains. Transcriptional profiling following Swi2 depletion also identified many previously known SWI/SNF-dependent genes, including *YOR222W, SER3,* and the acid phosphatase genes (Figure 4C). Notably, genes involved in ribosome biogenesis were not identified in the anchor away datasets, consistent with the possibility that expression of these genes are linked to growth rates. To identify genes that might be co-regulated by Swi2 and Sir3, we again selected genes that changed by 1.5 fold or more after depletion of *SWI2-FRB*, and performed hierarchical clustering to identify subsets that are co-regulated by *sir3*Δ. Genes that *decrease* (LFC < -0.58) in *SWI2*-FRB and were restored to nearly wild type levels in the *SWI2*-FRB *sir3*Δ were defined as Group 1_AA (Figure 4C; Table S2). The top GO term category enriched in Group 1_AA is ion/ carbohydrate transport and primarily reflects the metabolic defects of *SWI2* mutants in carbon source utilization. The overlap between the Group1_AA and Group1_KO sets revealed a very select set of 28 genes that decrease following loss of SWI/SNF but are restored to nearly wildtype levels by inactivation of Sir3 (p-value of 8.7×10^{-9} ; Figure 5C; Hypergeometric test). This common subset of genes, consolidated as Group 1, corresponds to GO term categories of 'cell cycle', 'cytokinesis', and 'lipid metabolism' (Table S3). Notably, this set is enriched for genes

298 expressed at the end of mitosis, which we previously showed to be SWI/SNF-dependent (Krebs, *et*
299 *al.* 2000).

300 Consistent with previous analyses, we also identified genes whose expression was
301 increased by either the deletion of *SWI2* or by Swi2 nuclear depletion (Figure S4). Expression of a
302 subset of these genes was restored to nearly wildtype levels by inactivation of Sir3, and these gene
303 sets were designated Group 2_KO (n= 488; LFC < -0.58 and FDR < 0.1) and Group 2_AA (n=
304 192; LFC < -0.58 and FDR < 0.1). (Figure 4B,C and S4A,B; Table S4 and S5). However, overlap
305 of Group 2_KO and Group 2_AA datasets revealed only 11 common genes (Figure S4C),
306 suggesting that the upregulation of genes by loss of SWI/SNF is primarily due to an indirect effect
307 of slow growth (Holstege *et al.* 1998b; Sudarsanam *et al.* 2000).
308
309 **Analysis of Sir3 binding at Group 1 target genes**
310 The genetic and transcriptome analyses suggest that SWI/SNF antagonizes Sir3 to promote
311 expression of specific genes. One prediction of this model is that Sir3 may accumulate at such
312 target genes in the absence of SWI/SNF. To test the model, we analyzed Sir3 recruitment by
313 chromatin immunoprecipitation (ChIP) in WT and *swi2*Δ mutants arrested in nocodazole.
314 Nocodazole is a microtubule depolymerizing agent that blocks entry into mitosis and thus, cells
315 accumulate at the G2/M border (Jacobs *et al.* 1988). Sir3 binding was measured using a native
316 antibody to Sir3, as well as an anti-FLAG antibody in a strain expressing a *SIR3*-FLAG fusion
317 from its endogenous locus. In both cases, ChIP analyses in the wild type strain demonstrated
318 enrichment for Sir3 at the heterochromatic loci, HMR and TELVI-R. In the absence of Swi2, the
319 occupancy of Sir3 is reduced at telomeres, consistent with a redistribution of Sir3 to ectopic loci

(Figure S5). However, we did not observe significant changes in Sir3 enrichment at selected euchromatic target genes (Figure S5B).

DISCUSSION:

Establishing a separation between euchromatin and heterochromatin domains is crucial for cell function. The mechanisms that might actively exclude heterochromatin proteins from euchromatin domains remain poorly understood. Previously, we found that the SWI/SNF complex can remove the Sir3 heterochromatin protein from chromatin fibers *in vitro*, and here, we report genetic evidence that supports a role for SWI/SNF in disrupting the ability of Sir heterochromatin proteins to repress euchromatic gene expression. In particular, this activity of SWI/SNF appears crucial for proper expression of genes expressed at the end of mitosis.

Genetic interactions between chromatin modifiers and *SIR* genes

Our *in vitro* studies indicated that the SWI/SNF chromatin remodeling enzyme was uniquely able to evict the Sir3 heterochromatin protein from chromatin fibers (Manning and Peterson 2014; Sinha *et al.* 2009). Here, we found that deletion of either *SIR3* or *SIR4* alleviated the growth defects of *swi2*Δ on media containing glucose, ethanol, or HU, but *sir3*Δ and *sir4*Δ did not significantly rescue the severe growth defects of *swi2*Δ on alternative carbon sources, such as raffinose or galactose. Likewise, inactivation of Sir proteins also alleviated the growth phenotypes of cells that were depleted of Swi2. Interestingly, the genetic interactions between genes encoding Sir proteins and SWI/SNF were not unique to this particular chromatin remodeler. Deletion of *SIR2* and *SIR3* also suppressed the growth defects of *ino80* and *hst3/hst4* mutants under genotoxic stress (Figure 2C, D), indicating a potential common mechanism for suppressing replication stress.

How does loss of Sir proteins alleviate the phenotypes of mutants that lack chromatin modifying enzymes? One possibility is that suppression is due to indirect effects caused by the pseudo-diploid state of *sir* mutant cells. Deletion of *SIR* genes induces the expression the a1-α2 repressor, generating pseudo-diploid cells. Such haploid cells expressing both *MAT* genes show greater resistance to radiation and are more recombination proficient than cells expressing only *MATα* or *MATa* (Heude and Fabre 1993). We found that pseudo-diploid cells partially suppressed the phenotypes of the *INO80-FRB* and *hst4Δ/HST3-FRB* strains to a similar level as deletion of *SIR* genes, especially for growth on CPT (Figure 3B,C), indicating the some genetic interactions between INO80C and Hst3/Hst4 with Sir proteins may be largely indirect. In contrast, although the pseudodiploid state partially suppressed the HU stress phenotype of the *SNF2-FRB* strain (Figure 3A), the suppression was much less than that observed after deletion of *SIR3* (Figure 2B). This suggests there exists both a direct genetic interaction between SWI/SNF and Sir3, consistent with the ability of SWI/SNF to evict Sir3 *in vitro* (Manning and Peterson 2014), as well as an indirect interaction caused by *MAT* heterozygosity.

Transcriptional profiling of *swi2*Δ and *swi2*Δ *sir3*Δ strains

Our transcriptional profiling data suggest that there may be at least two classes of SWI/SNF-dependent genes – those where SWI/SNF antagonizes Sir proteins, and a second group of genes that may require more "canonical" nucleosome remodeling activities. Our transcriptional profiling results are consistent with this view, as we identified many SWI/SNF-dependent genes whose transcriptional defect was not restored by loss of Sir3 and a separate set of genes where SWI/SNF appears to antagonize Sir3. Furthermore, we recently identified and characterized a separation of function allele of *SWI2* (*swi2*Δ-Δ*10R*) that generates a SWI/SNF complex that has

366 normal levels of nucleosome remodeling activity but lacks the ability to evict Sir3 from chromatin
367 fibers. (Manning and Peterson 2014).

368 For genes where SWI/SNF appears to antagonize Sir3, our microarray analyses revealed
369 two categories of genes – the first group includes ribosomal biogenesis and ribosomal protein
370 coding genes and the second include genes involved in cytokinesis and cell division. Notably, the
371 first category of genes are likely to be sensitive to growth rate and thus changes in their expression
372 are most likely due to indirect effects (Airoldi *et al.* 2009) (Figure 5C). In contrast, genes involved
373 in mitotic exit were identified in RNA profiles from both gene deletion strains and from the anchor
374 away system. This suggest that defects in expression of these genes are likely to be independent of
375 the growth defects of the swi2 deletion strain and may be direct targets where SWI/SNF
376 antagonizes Sir3. These data lend mechanistic insight to previous findings that SWI/SNF promotes
377 expression of genes involved in mitotic exit and that *SWI/SNF* mutants are defective in exiting
378 mitosis (Krebs *et al.* 2000).
379

380 **Genes expressed during mitosis are dependent on SWI/SNF to antagonize Sir3**

381 Why might Sir3 only impact genes that are expressed during mitosis? Cytological studies have
382 shown that Sir3 localizes to discrete foci during the majority of the cell cycle, reflecting its
383 heterochromatic localization (Laroche *et al.* 2000). In contrast, Sir3 shows a diffuse, nuclear
384 staining pattern during mitosis, consistent with more promiscuous binding to both euchromatic and
385 heterochromatic sites. However, we do not observe increased Sir3 occupancy at selected gene
386 promoter regions by ChIP qPCR analyses in G2/M arrested cells, compared to asynchronous cell
387 populations (Figure S5B), though a diffuse localization of Sir3 may not be detectable by ChIP-
388 qPCR. Likewise, we did not detect changes in euchromatic Sir3 occupancy in the absence of

389 SWI/SNF, though Sir3 levels were decreased from telomeric regions, consistent with previous
390 reports (Dror and Winston 2004; Manning and Peterson 2014) (Figure S5). Currently, we favor a
391 model in which Sir3 delocalizes from heterochromatic sites during mitosis, leading to the binding
392 of Sir3 to euchromatic regions, perhaps facilitated by the deacetylated state of transcribed gene
393 coding regions. Sir3 may bind in a diffuse manner across euchromatic genes, limiting the detection
394 of Sir3 by ChIP analyses. We envision that SWI/SNF action may be required to remove Sir3,
395 facilitating expression of these cell cycle regulated genes. Notably, this role for SWI/SNF would
396 be distinct from the typical nucleosome remodeling activities of SWI/SNF.
397

ACKNOWLEDGEMENTS

We thank Phyllis Spatrick and the Genomics Core Facility at UMass Medical School for assistance with sample processing. The pJR156 and pJR157 *MAT* plasmids were a gift from Prof. Jasper Rine at the University of California, Berkeley. This work was supported by grants from the NIH to C.L.P. (R35 GM122519) and to J.L.F. (F32 GM119229).

404 **REFERENCES:**

405 Abrams, E., Neigeborn, L., and Carlson, M. (1986). Molecular analysis of SNF2 and SNF5, genes
406 required for expression of glucose-repressible genes in Saccharomyces cerevisiae. Mol. Cell.
407 Biol. *6*, 3643–3651.

408 Airoldi, E.M., Huttenhower, C., Gresham, D., Lu, C., Caudy, A.A., Dunham, M.J., Broach, J.R.,
409 Botstein, D., and Troyanskaya, O.G. (2009). Predicting cellular growth from gene expression
410 signatures. PLoS Comput. Biol. *5*, e1000257.

411 Bennett, G., Papamichos-Chronakis, M., and Peterson, C.L. (2013). DNA repair choice defines a
412 common pathway for recruitment of chromatin regulators. Nat. Commun. *4*, 2084.

413 Carlson, M., Osmond, B. C., & Botstein, D. (1981). Mutants of yeast defective in sucrose
414 utilization. Genetics, *98*, 25–40.

415 Carmen, A.A., Milne, L., and Grunstein, M. (2002). Acetylation of the yeast histone H4 N
416 terminus regulates its binding to heterochromatin protein SIR3. J Biol Chem *277*, 4778–4781.

417 Carrozza, M.J., Li, B., Florens, L., Suganuma, T., Swanson, S.K., Lee, K.K., Shia, W.-J.,
418 Anderson, S., Yates, J., Washburn, M.P., *et al.* (2005). Histone H3 methylation by Set2 directs
419 deacetylation of coding regions by Rpd3S to suppress spurious intragenic transcription. Cell
420 *123*, 581–592.

421 Clapier, C.R., and Cairns, B.R. (2009). The biology of chromatin remodeling complexes. Annu.
422 Rev. Biochem. *78*, 273–304.

423 Dranginis, A. M. (1990). Binding of yeast a1 and alpha 2 as a heterodimer to the operator DNA of
424 a haploid-specific gene. Nature *347*, 682-685.

425 Dror, V., and Winston, F. (2004). The Swi / Snf Chromatin Remodeling Complex Is Required for
426 Ribosomal DNA and Telomeric Silencing in Saccharomyces cerevisiae. *24*, 8227–8235.

427 Goutte, C., and A. D. Johnson. (1988). a1 protein alters the DNA binding specificity of alpha 2
428 repressor. Cell *52,* 875-882.

429 Haber J.E. (1998). Mating-type gene switching in Saccharomyces cerevisiae. Annu Rev Genet.
430 1998;32:561-99.

431 Haruki, H., Nishikawa, J., and Laemmli, U.K. (2008). The anchor-away technique: rapid,
432 conditional establishment of yeast mutant phenotypes. Mol. Cell *31*, 925–932.

433 Herskowitz, I. (1989). A regulatory hierarchy for cell specialization in yeast. Nature *342,* 749-757.

434 Heude, M., & Fabre, F. (1993). a/alpha-control of DNA repair in the yeast Saccharomyces
435 cerevisiae: genetic and physiological aspects. Genetics *133*, 489–498.

436 Holmes, S.G., Rose, A.B., Steuerle, K., Saez, E., Sayegh, S., Lee, Y.M., and Broach, J.R. (1997).
437 Hyperactivation of the silencing proteins, Sir2 and Sir3, causes chromosome loss. Genetics
438 *145*, 605–614.

439 Holstege, F.C., Jennings, E.G., Wyrick, J.J., Lee, T.I., Hengartner, C.J., Green, M.R., Golub, T.R.,
440 Lander, E.S., and Young, R.A. (1998a). Dissecting the regulatory circuitry of a eukaryotic
441 genome. Cell *95*, 717–728.

442 Holstege, F.C.., Jennings, E.G., Wyrick, J.J., Lee, T.I., Hengartner, C.J., Green, M.R., Golub, T.R.,
443 Lander, E.S., and Young, R.A. (1998b). Dissecting the Regulatory Circuitry of a Eukaryotic
444 Genome. Cell *95*, 717–728.

445 Jacobs, C.W., Adams, A.E., Szaniszlo, P.J., and Pringle, J.R. (1988). Functions of microtubules in

the Saccharomyces cerevisiae cell cycle. J. Cell Biol. *107*, 1409–1426.

Keogh, M.-C., Kurdistani, S.K., Morris, S. a, Ahn, S.H., Podolny, V., Collins, S.R., Schuldiner, M., Chin, K., Punna, T., Thompson, N.J., *et al.* (2005). Cotranscriptional set2 methylation of histone H3 lysine 36 recruits a repressive Rpd3 complex. Cell *123*, 593–605.

Krebs, J.E., Fry, C.J., Samuels, M.L., and Peterson, C.L. (2000). Global role for chromatin remodeling enzymes in mitotic gene expression. Cell *102*, 587–598.

Laroche, T., Martin, S.G., Tsai-Pflugfelder, M., and Gasser, S.M. (2000). The dynamics of yeast telomeres and silencing proteins through the cell cycle. J. Struct. Biol. *129*, 159–174.

Laurent, B. C., Treitel, M. A., & Carlson, M. (1991). Functional interdependence of the yeast SNF2, SNF5, and SNF6 proteins in transcriptional activation. Proc Natl Acad Sci U S A. *88*, 2687–2691.

Lenstra, T.L., Benschop, J.J., Kim, T., Schulze, J.M., Brabers, N. a C.H., Margaritis, T., van de Pasch, L. a L., van Heesch, S. a a C., Brok, M.O., Groot Koerkamp, M.J. a, *et al.* (2011). The Specificity and Topology of Chromatin Interaction Pathways in Yeast. Mol. Cell *42*, 536–549.

Manning, B.J., and Peterson, C.L. (2014). Direct interactions promote eviction of the Sir3 heterochromatin protein by the SWI/SNF chromatin remodeling enzyme. Proc. Natl. Acad. Sci. U. S. A. *111*, 17827–17832.

Peterson, C.L. and Herskowitz, I. (1992). Characterization of the yeast SWI1, SWI2, and SWI3 genes, which encode a global activator of transcription. Cell *68*, 573-83.

Radman-Livaja, M., Ruben, G., Weiner, A., Friedman, N., Kamakaka, R., and Rando, O.J. (2011). Dynamics of Sir3 spreading in budding yeast: secondary recruitment sites and euchromatic

localization. EMBO J. *30*, 1012–1026.

Rege, M., Subramanian, V., Zhu, C., Hsieh, T. H., Weiner, A., Friedman, N., Clauder-Münster, S., Steinmetz, L. M., Rando, O. J., Boyer, L. A., & Peterson, C. L. (2015). Chromatin Dynamics and the RNA Exosome Function in Concert to Regulate Transcriptional Homeostasis. Cell Rep. *13*, 1610–1622.

Richmond, E., and Peterson, C.L. (1996). Functional analysis of the DNA-stimulated ATPase domain of yeast SWI2/SNF2. Nucleic Acids Res *24*, 3685–3692.

Rine, J., & Herskowitz, I. (1987). Four genes responsible for a position effect on expression from HML and HMR in Saccharomyces cerevisiae. Genetics *116*, 9–22.

Rusche, L.N., Kirchmaier, A.L., and Rine, J. (2003). The establishment, inheritance, and function of silenced chromatin in Saccharomyces cerevisiae. Annu Rev Biochem *72*, 481–516.

Rusché, L.N., Kirchmaier, A.L., and Rine, J. (2002). Ordered nucleation and spreading of silenced chromatin in Saccharomyces cerevisiae. Mol Biol Cell *13*, 2207–2222.

Schild, D. (1995). Suppression of a new allele of the yeast RAD52 gene by overexpression of RAD51, mutations in srs2 and ccr4, or mating-type heterozygosity. Genetics *140,* 115-127.

Schwabish, M.A., and Struhl, K. (2007). The Swi/Snf complex is important for histone eviction during transcriptional activation and RNA polymerase II elongation in vivo. Mol Cell Biol *27*, 6987–6995.

Sharma, V.M., Li, B., and Reese, J.C. (2003). SWI/SNF-dependent chromatin remodeling of RNR3 requires TAF(II)s and the general transcription machinery. Genes Dev. *17*, 502–515.

Sinha, M., Watanabe, S., Johnson, A., Moazed, D., and Peterson, C.L. (2009). Recombinational

repair within heterochromatin requires ATP-dependent chromatin remodeling. Cell *138*, 1109–1121.

Smith, C.L., and Peterson, C.L. (2005). ATP-dependent chromatin remodeling. Curr Top Dev Biol *65*, 115–148.

Sudarsanam, P., Iyer, V.R., Brown, P.O., and Winston, F. (2000). Whole-genome expression analysis of snf/swi mutants of Saccharomyces cerevisiae. Proc Natl Acad Sci U S A *97*, 3364–3369.

Taddei, A., Van Houwe, G., Nagai, S., Erb, I., van Nimwegen, E., and Gasser, S.M. (2009). The functional importance of telomere clustering: global changes in gene expression result from SIR factor dispersion. Genome Res *19*, 611–625.

Thurtle, D.M., and Rine, J. (2014). The molecular topography of silenced chromatin in Saccharomyces cerevisiae. Genes Dev. *28*, 245–258.

Valencia-Burton, M., Oki, M., Johnson, J., Seier, T. A., Kamakaka, R., & Haber, J. E. (2006). Different mating-type-regulated genes affect the DNA repair defects of Saccharomyces RAD51, RAD52 and RAD55 mutants. Genetics *174*, 41–55.

Welch, E., Barton ER, Zhuo J, Tomizawa Y, Friesen WJ, Trifillis P, Paushkin S, Patel M, Trotta CR, Hwang S, *et al.* (2007). PTC124 targets genetic disorders caused by nonsense mutations. Nature *447*, 87-91.

Wilson, C.J., Chao, D.M., Imbalzano, A.N., Schnitzler, G.R., Kingston, R.E., and Young, R.A. (1996). RNA polymerase II holoenzyme contains SWI/SNF regulators involved in chromatin remodeling. Cell *84*, 235–244.

509 **FIGURE LEGENDS:**

510 **Figure 1: *swi2* growth defects are partially rescued by deletion of *SIR3***

511 A) Tetrad dissection plates of the *swi2*Δ*/SWI2 sir3*Δ*/SIR3* heterozygous diploid on YEPD plates
512 with the corresponding genotypes marked with symbols listed on the left. A single dissected spore
513 yields an isogenic colony, imaged after 10 days. Relative size of each colony is representative of the
514 growth rate.

515 B) Spot assay on null mutants dissected from the W303 background. Equal cell numbers were
516 spotted in consecutive ten-fold dilutions on agar plates with 2% glucose as the carbon source and
517 imaged after 3 days.

518 C) Spot assay was performed as described in B) with different carbon sources. Raffinose and
519 galactose plates also contain 2% antimycin to prevent respiratory growth.

520 D) *swi2*Δ *sir3*Δ mutants transformed with a plasmid containing either the vector backbone (left) or
521 with a construct expressing Sir3 from its endogenous promoter (right). Spot assays were performed
522 on individual isolates as described in B).

523

524
525

Figure 2: Absence of Sir2 *or* Sir3 partially suppresses phenotypes due to depletion of SWI/SNF, Hst3/Hst4, or INO80C

A) Schematic of the Anchor-away system to induce conditional depletion of nuclear proteins. Strains contain C-terminally tagged versions of the nucleo-cytoplasmic shuttling protein (*RPL13A-FKBP12;* green hook) and the *SWI2* gene locus (*SWI2-FRB;* yellow star) (left panel). Addition of Rapamycin (red dot) facilitates formation of a ternary complex between FKBP12 and FRB, rapidly depleting *SWI2-FRB* from the nucleus (right panel).

B) Wild type, *sir2*Δ, and *sir3*Δ strains with or without the *SWI2*-FRB tag were spotted on 2% glucose media containing either DMSO solvent, 8µg/ml rapamycin (RAP) in the presence or absence of 0.1 M hydroxyurea (HU) and then grown for 3 days at 30˚C.

C) Spot assays as in B) for *hst4*Δ*/HST3-FRB* in the presence of or absence 0.1 M HU and 5 µg/mL Camptothecin (CPT).

D) Spot assays as in B) for *INO80-FRB* in the presence or absence of 0.1 M HU and 5 µg/mL CPT.

Figure 3: *MAT* heterozygosity partially suppresses replication stress phenotypes due to depletion of chromatin regulators

A) *SNF2*-FRB tag strains containing either empty vector or a vector expressing *MATa* were spotted on 2% glucose media containing either DMSO solvent, 8µg/ml rapamycin (RAP) in the presence or absence of 5 µg/mL Camptothecin (CPT) and 0.1 M HU, and then grown for 3 days at 30˚C. Two transformants were tested.

B) Spot assays as in A) for *hst4*Δ*/HST3-FRB* expressing *MATα* grown in the presence or absence of 5 µg/mL CPT and 0.1 M HU .

C) Spot assays as in A) for *INO80-FRB* expressing *MATα* grown in the presence or absence of 5 µg/mL CPT and 0.1 M HU .

554 **Figure 4: Whole-genome microarray analysis of *swi2*Δ and *SWI2*-AA strains.**

555 A) Volcano plots show transcripts that change significantly in the mutant compared to the wild type
556 (WT) highlighted in blue (p.adj = FDR < 0.1 and Log_2 Fold Change > 0.59).

557 B) Heatmap of normalized RNA abundance for ORFs that are significantly down-regulated (n= 167)
558 and up-regulated (n=488) in the *swi2*Δ arrays compared to WT. Corresponding values for these
559 genes from *swi2Δ sir3Δ* and *sir3Δ* arrays compared to WT are also shown. Group 1_KO are defined
560 as significantly down-regulated in the *swi2*Δ and comparatively de-repressed in *swi2*Δ *sir3*Δ, while
561 Group 2_KO are defined as significantly up-regulated in the *swi2*Δ and comparatively reduced in
562 *swi2*Δ *sir3*Δ. Examples of ORFs identified in previous studies that do not change in *swi2*Δ *sir3*Δ
563 compared to *swi2*Δ (> ± 1.5 fold) are listed along the right.

564 C) Heatmap of normalized RNA abundance for genes that are down-regulated (n=264) and up-
565 regulated (n=193) in the *SWI2*-FRB compared to WT in the presence of 8µg/ ml of rapamycin
566 (RAP). Corresponding values for these genes from *SWI2-FRB sir3Δ* and *sir3Δ* arrays compared to
567 WT are also shown. 'Group 1_AA' and 'Group 2_AA' are defined essentially as described in B).
568 Examples of ORFs identified in previous studies that do not change in *swi2*Δ *sir3*Δ compared to
569 *swi2*Δ (> ± 1.5 fold) are listed along the right.

570

Figure 5: M/G1 expressed genes are regulated by SWI/SNF in a Sir3 dependent manner in both the *SWI2* anchor-away and *swi2Δ* strains

A) Heatmap of normalized RNA abundance for Group1_AA ORFs (n= 263) in the *SWI2-FRB*, *SWI2-FRB sir3Δ* and *sir3Δ* arrays compared to WT in the presence of 8µg/ ml of rapamycin (RAP) after hierarchical clustering.

B) Heatmap of normalized RNA abundance for Group1_KO ORFs (n= 176) in the *swi2*Δ, *swi2Δ sir3Δ* and *sir3Δ* arrays compared to WT after hierarchical clustering.

C) Venn diagram depicting the overlap of genes from Group 1_AA and Group 1_KO. GO terms specific and common to the knockout (KO) and anchor-away (AA) datasets are shown.

D) RT-qPCR analysis of select Group 1 genes identified from both the knockout and anchor-away datasets sets.

583 **Figure S1: Gene expression and genetic interactions of *SIR3*, *SIR2,* and *SIR4* with *SWI2*.**

584 A, B) Absence of *SIR2* does not suppress growth defects of *swi2*Δ.

585 C, D) Absence of *SIR4* suppresses the growth defects of *swi2*Δ.

586 E) Absence of *SIR3* does not impact *RNR* gene expression and genetic interactions.
587

588 **Figure S2: *ino80* growth defects are partially rescued by deletion of *SIR3***

589 A) Tetrad dissection plates of the *ino80*Δ*/INO80 sir3*Δ*/SIR3* heterozygous diploid on YEPD plates
590 with the corresponding genotypes marked with symbols listed on the right. A single dissected spore
591 yields an isogenic colony, imaged after 10 days. Relative size of each colony is representative of the
592 growth rate.

593 B) Spot assay on null mutants dissected from the W303 background. Equal cell numbers were
594 spotted in consecutive ten-fold dilutions on agar plates with 2% glucose as the carbon source in the
595 presence or absence of 0.05 M HU, 0.1 M HU, 0.01% Methyl methanesulfonate (MMS), 0.03%
596 MMS, 30 µg/mL CPT, 90 µg/mL CPT, 2.5 µg/mL phleomycin, or 5 µg/mL phleomycin and imaged
597 after 3 days.

598

599

Figure S3: *G*rowth defects due to depletion of chromatin regulators are not suppressed by deletion of haploid-specific genes *NEJ1*, *RME1*, or *PST2*

A) Wild type and *nej1*Δ strains with or without the *SNF2*-FRB, *hst4*Δ*/HST3-FRB*, or *INO80-FRB* were spotted (1/10 dilutions) on 2% glucose media containing either DMSO solvent, 8µg/ml rapamycin (RAP) in the presence or absence of 0.1 M HU and 5 µg/mL Camptothecin (CPT). Cells were then grown for 3 days at 30˚C.

B) Spot assays as in A) for *rme1*Δ.

C) Spot assay as in A) for *pst2*Δ.

Figure S4: Overlap of Group 2 genes (those repressed by *SWI2*) between *swi2Δ* and *SWI2* anchor-away strains

A) Group 2_KO (n= 192) heatmap with strains compared to WT anchor away strain.

B) Group 2_AA (n=488) heatmap with null mutants compared to WT.

C) Overlap of the number of genes from Group 2_AA and Group 2_KO and the corresponding GO term categories.

Figure S5: ChIP analysis of Sir3 occupancy

A) Chromatin immunoprecipitation (ChIP) for native Sir3 in nocodazole-arrested (G2/M boundary) cells at two heterochromatic loci in WT, *sir3*Δ and *swi2*Δ cells.

B) ChIP for *SIR3*-FLAG in nocodazole-arrested (G2/M boundary) cells at promoters of *SWI2* dependent genes in WT and *swi2*Δ cells.

SUPPLEMENTARY TABLES

Table S1: List of Group 1_KO genes

Table S2: List of Group 1_AA genes

Table S3: List of Group 1 genes common in the KO and AA datasets

Table S4: List of Group 2_KO genes

Table S5: List of Group 2_AA genes

Table S6: Complete table of RMA values from the KO datasets for all genes

Table S7: Complete table of RMA values from the AA datasets for all genes

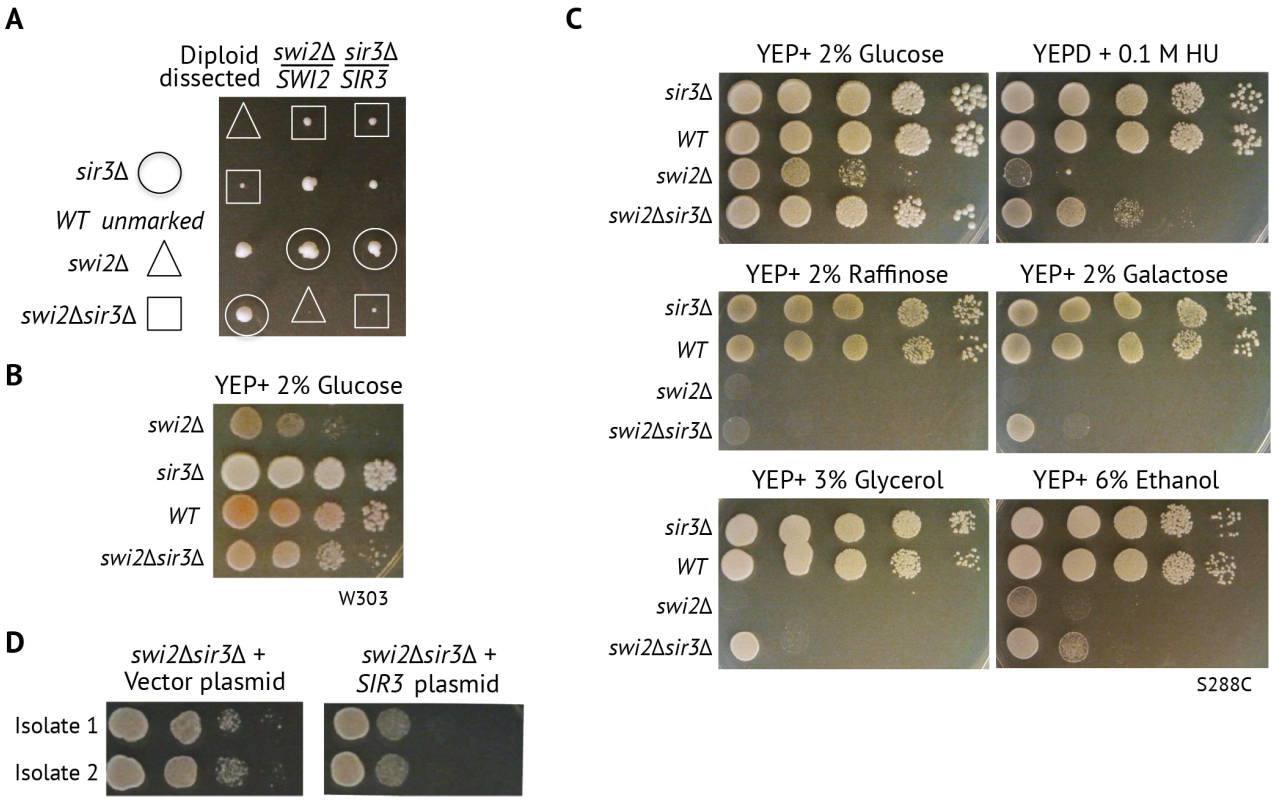

A

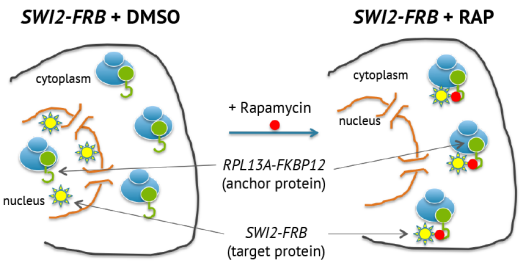

B

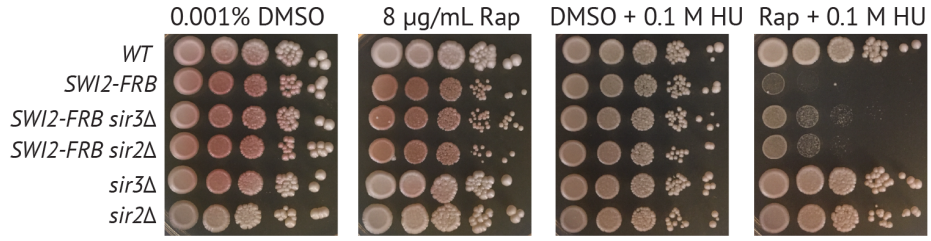

C

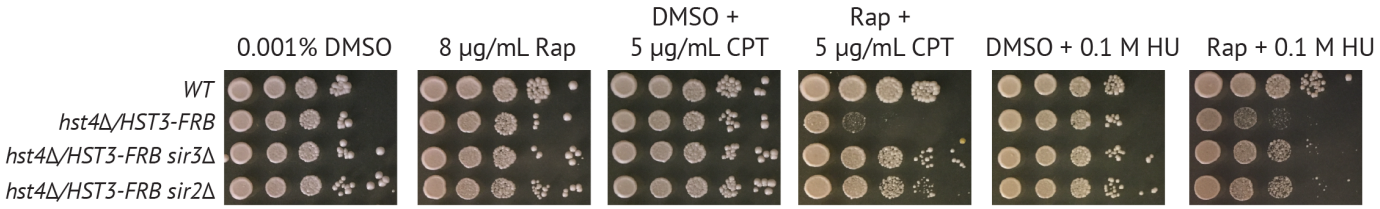

D

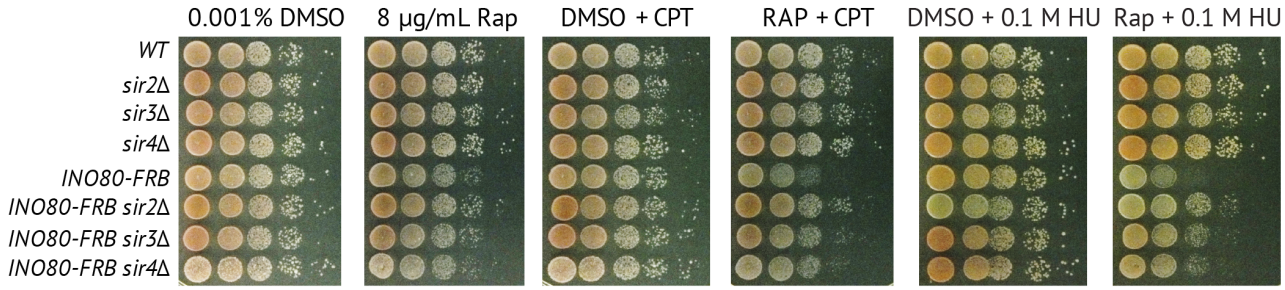

A

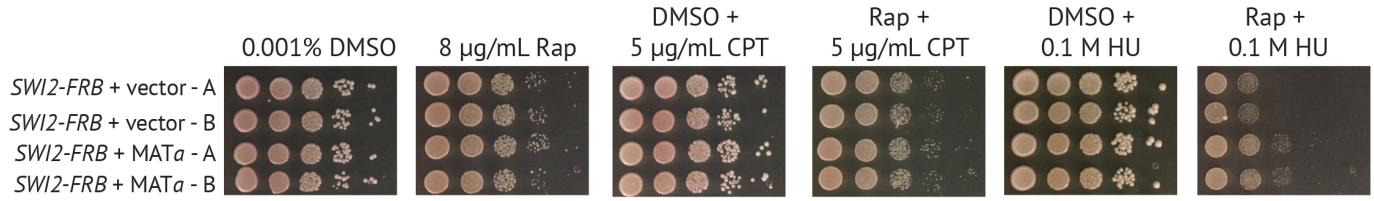

B

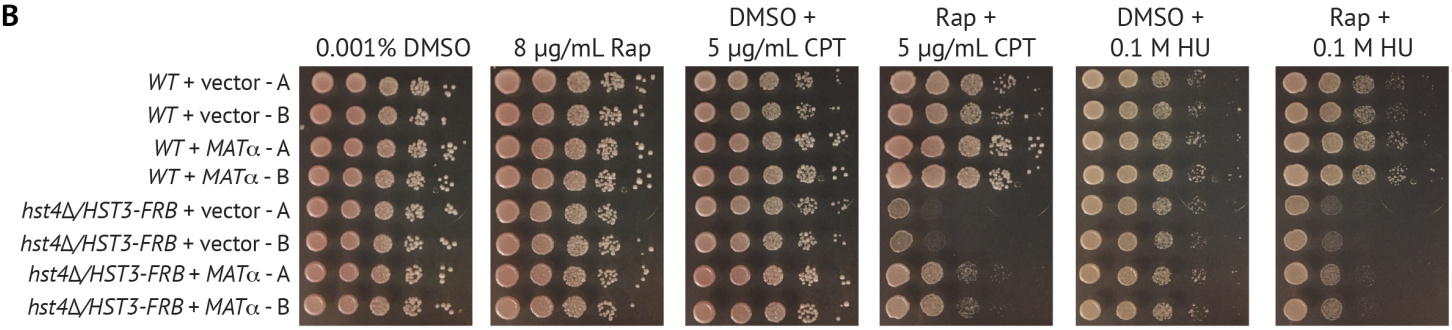

C

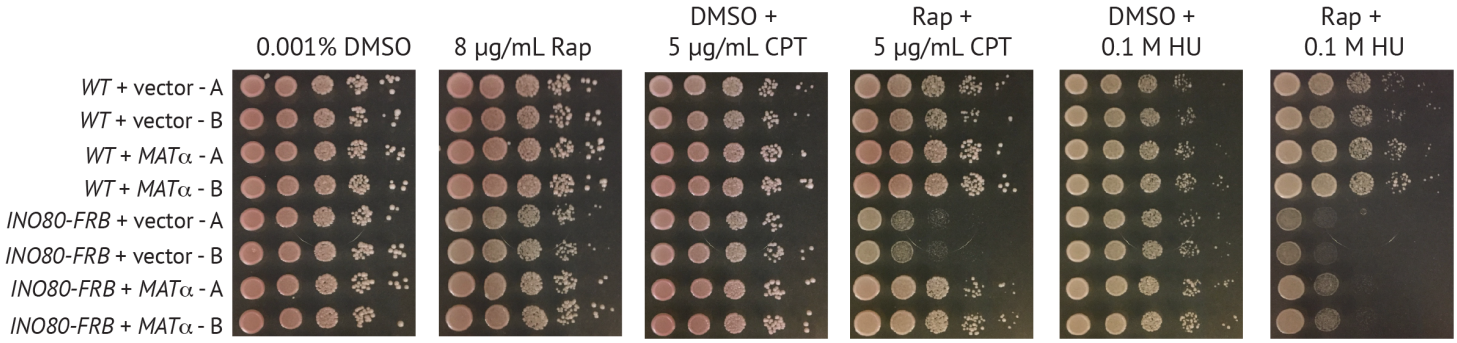

Figure 4

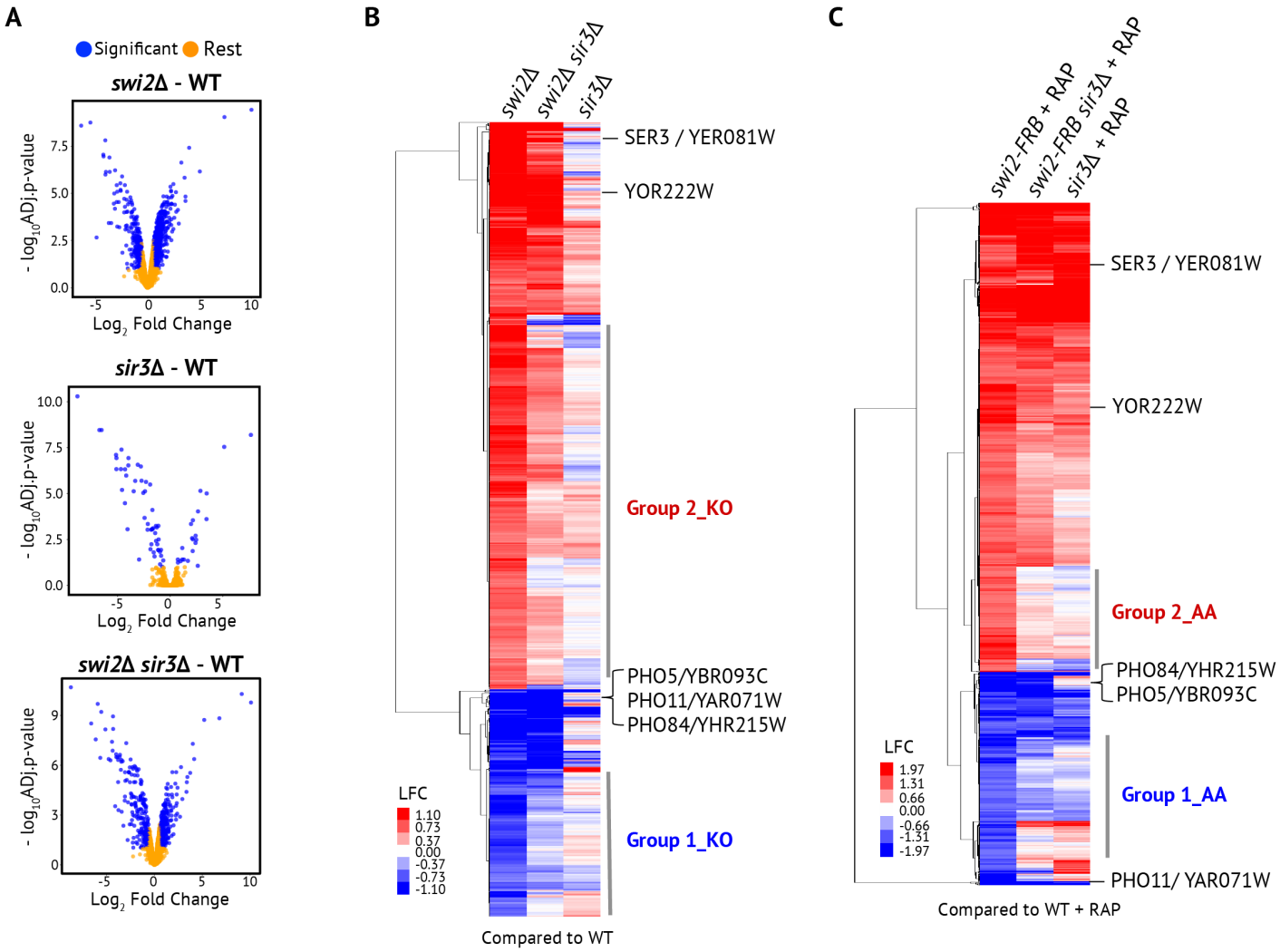

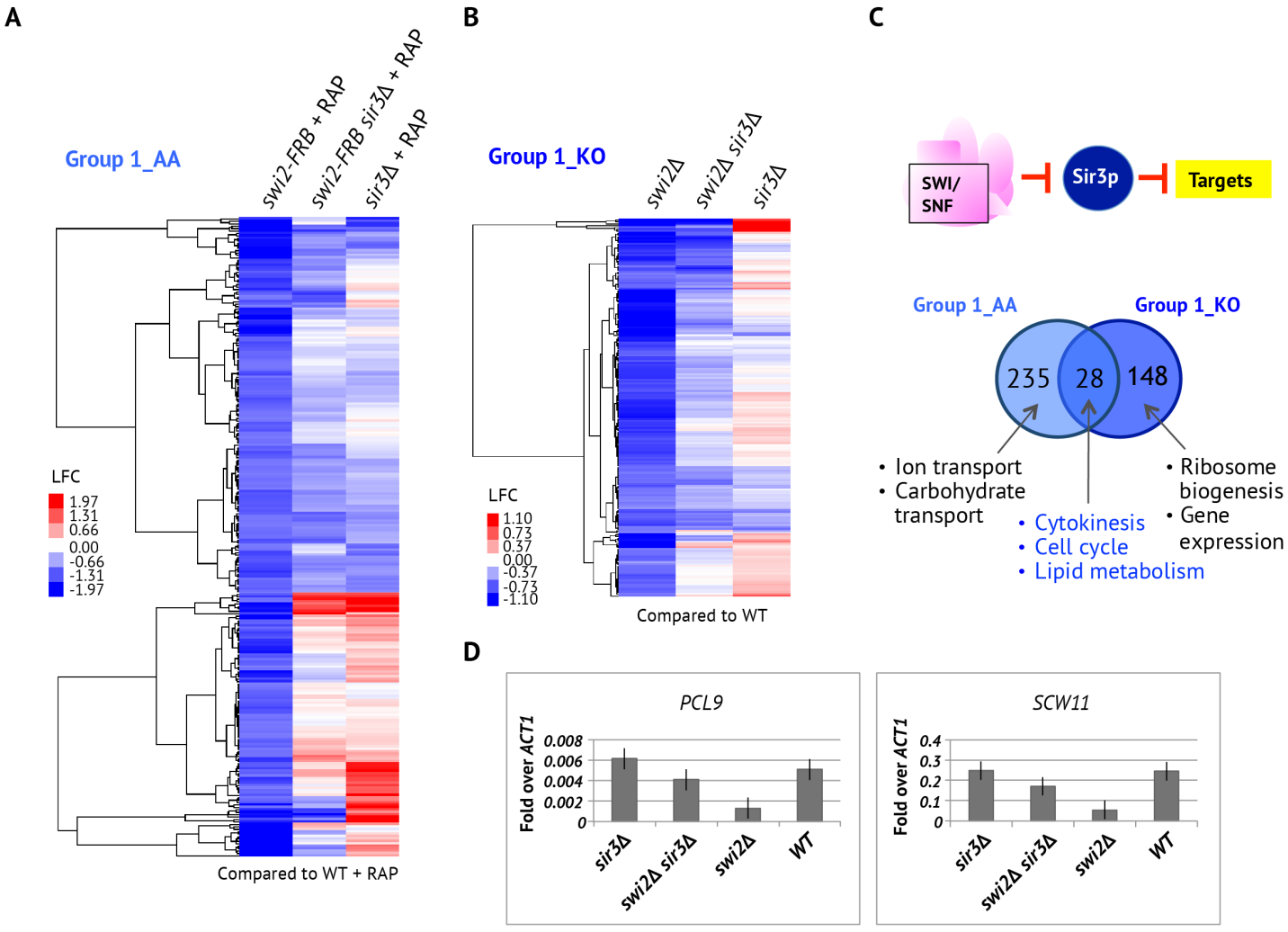

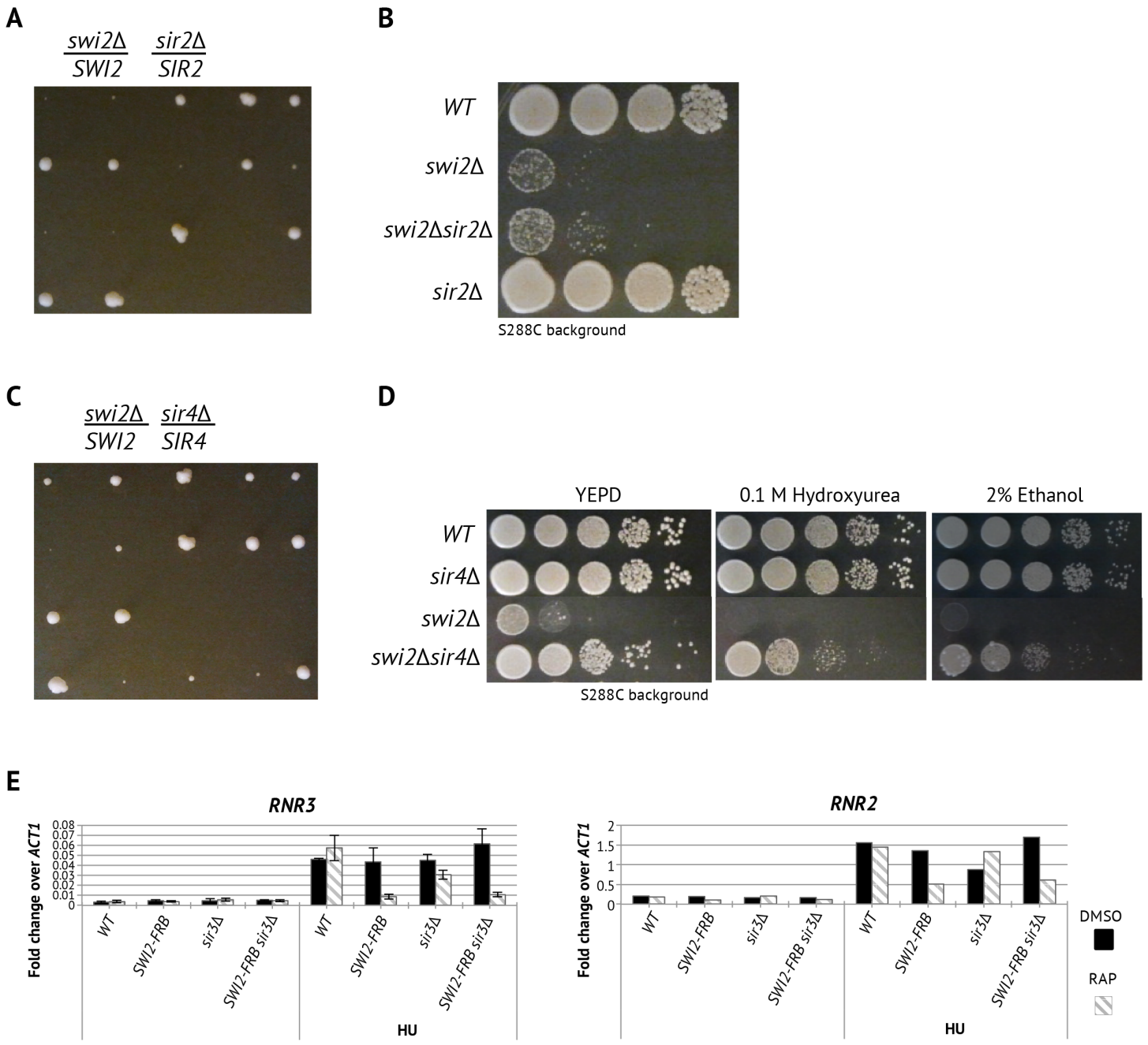

A

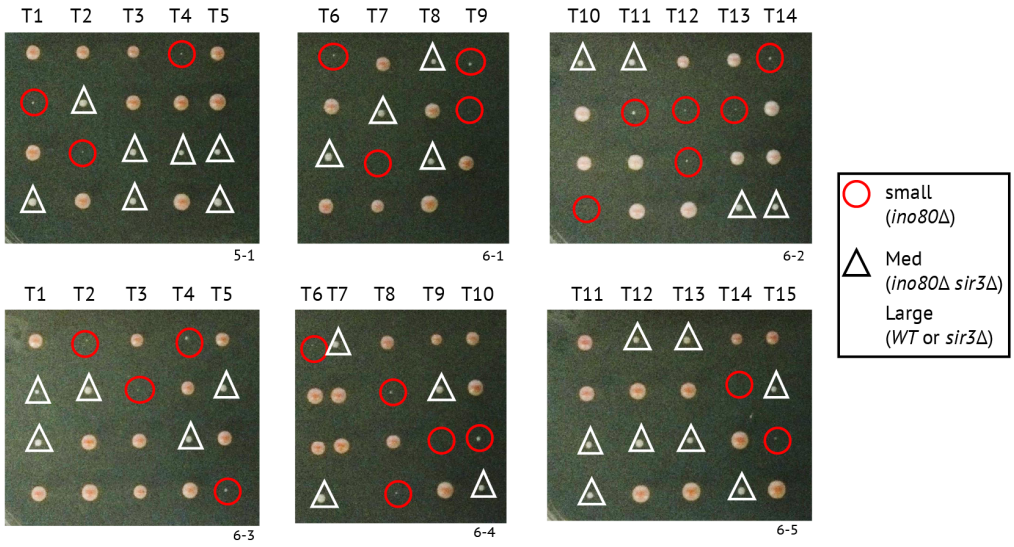

B

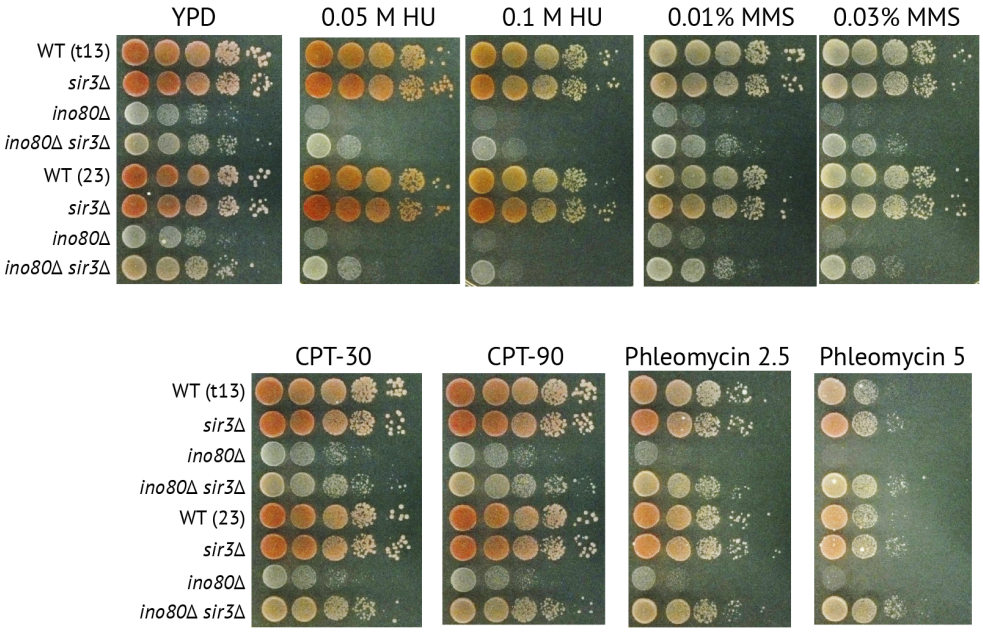

A

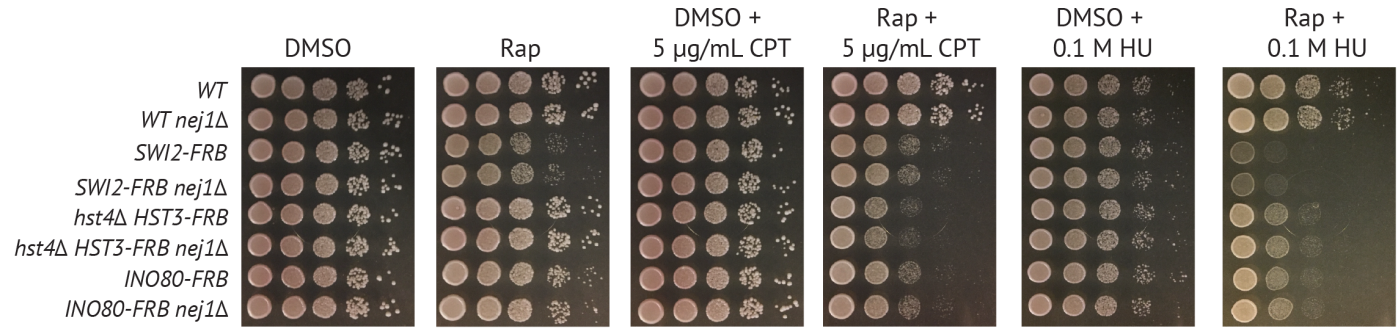

B

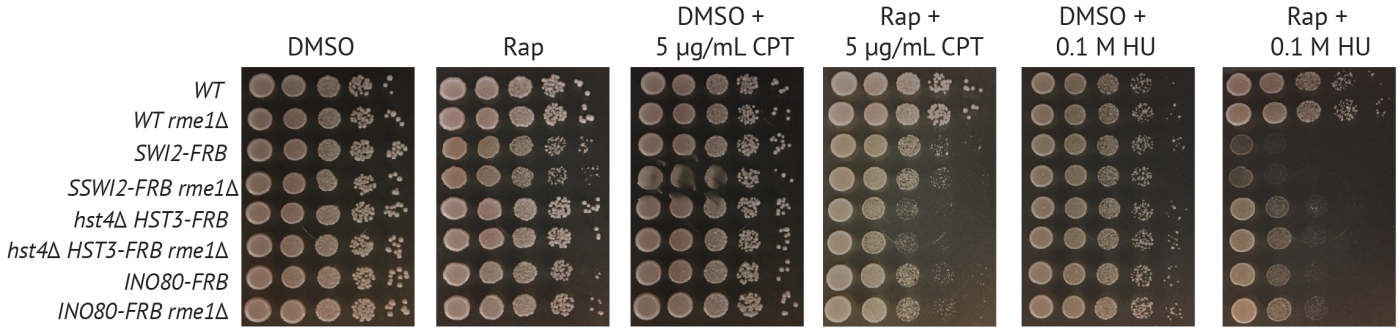

C

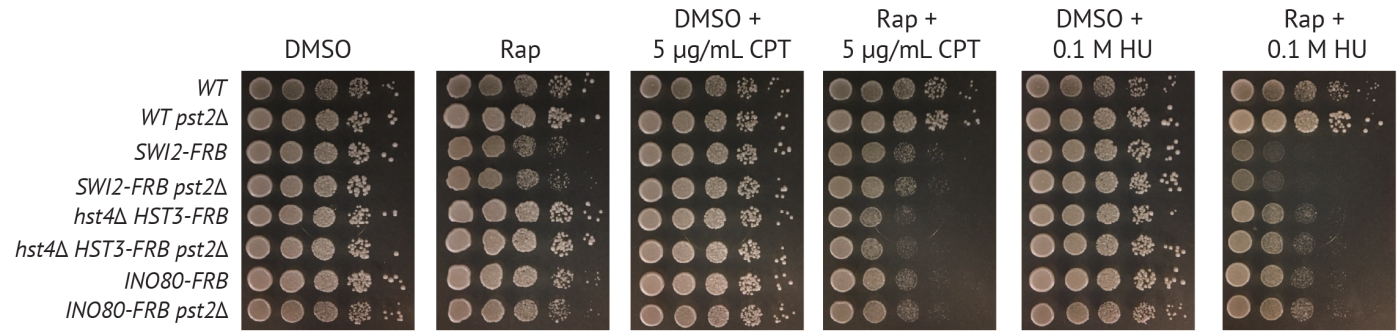

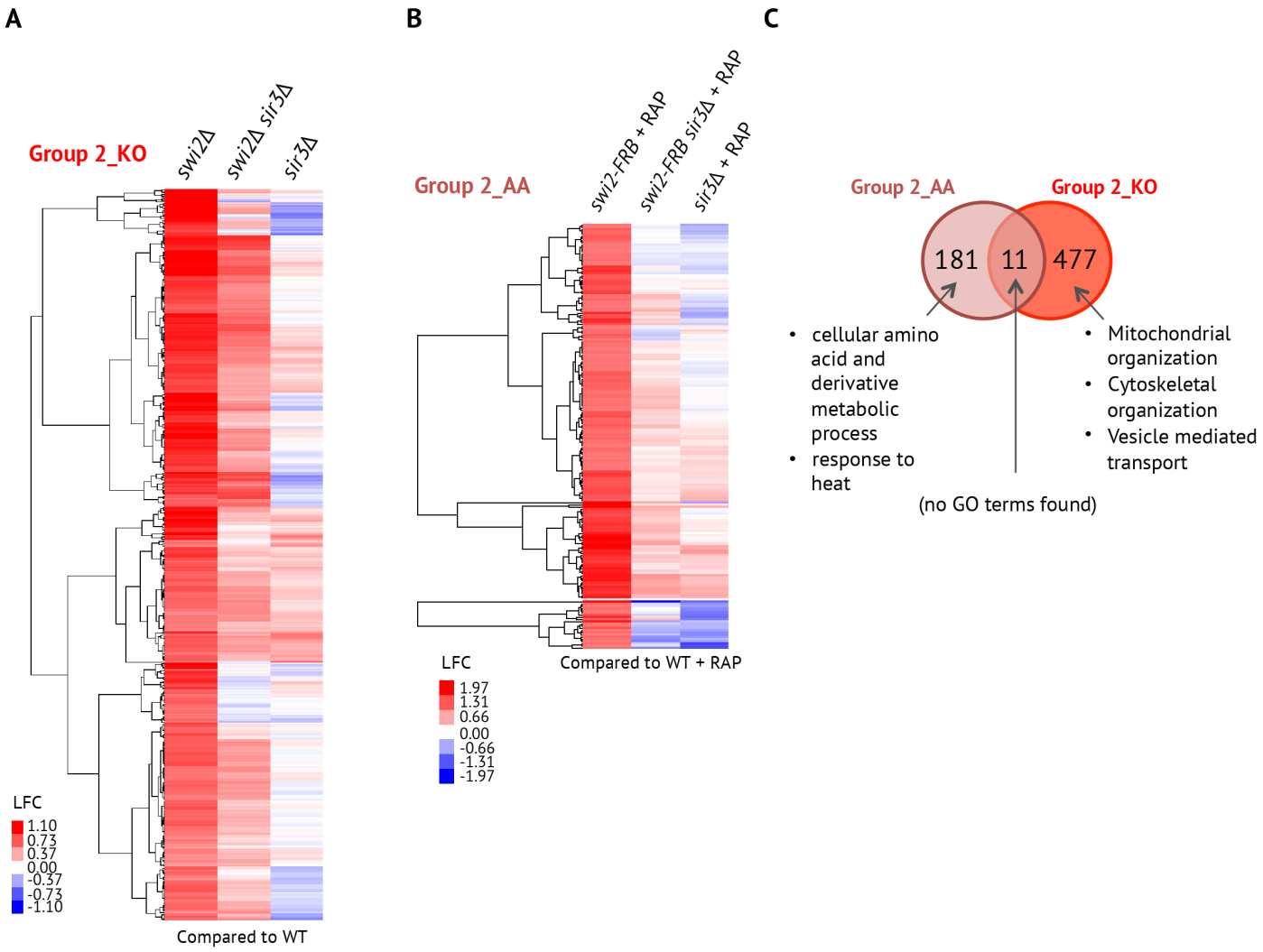

A

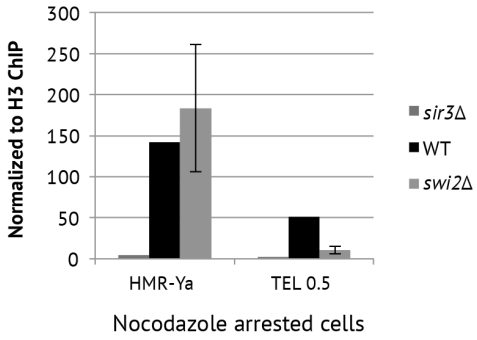

B

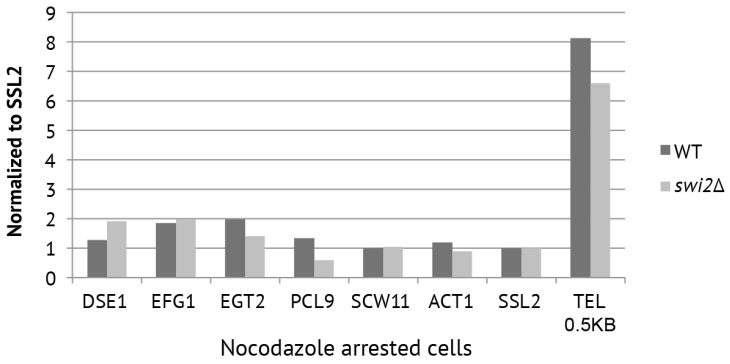

Table S1. List of Group 1 KD genes

swi2D = swi2 null mutant; sir3D = sir3 null mutant, WT = Wildtype

YORF	NAME	swi2D-WT	swi2Dsir3D-WT	sir3D-WT
YOR107W	YOR107W	-1.736286	-1.249234	0.802684
YOR049C	YOR049C	-1.799513	-1.528723	1.077021
YOR032C	YOR032C	-1.190089	-1.02068	1.545266
YJL116C	YJL116C	-2.189504	-0.596606	2.268662
YIL169C	YIL169C	-0.686039	-0.35075	2.457973
YIL169C	YIL169C	-0.866575	-0.786447	2.38699
YOL155C	YOL155C	-0.771853	-0.763125	2.132386
YLL012W	YLL012W	-1.095636	-0.664814	0.251892
YMR182W-A	YMR182W	-1.19808	-0.661026	0.069504
YER072W	YER072W	-1.036205	-0.931685	-0.004959
YBR238C	YBR238C	-1.113228	-1.032084	0.050758
YGR079W	YGR079W	-1.056979	-0.935159	0.135865
YNL141W	YNL141W	-1.263049	-0.889395	0.046825
YKL185W	YKL185W	-0.871451	-0.845494	-0.158825
YHR049W	YHR049W	-0.982429	-0.822014	-0.31239
YER062C	YER062C	-0.938457	-0.793679	-0.232057
YOL002C	YOL002C	-0.883949	-0.611531	-0.186142
YOR101W	YOR101W	-0.89683	-0.624431	-0.017271
YLR008C	YLR008C	-0.812653	-0.574562	-0.044313
YFL004W	YFL004W	-0.986432	-0.698759	0.025827
YBR085W	YBR085W	-1.020654	-0.603666	-0.067401
YDR384C	YDR384C	-0.95195	-0.607941	0.163866
YJR060W	YJR060W	-0.792775	-0.641355	0.115003
YPR054W	YPR054W	-0.786343	-0.572491	0.119735
YLR300W	YLR300W	-0.593589	-0.854639	0.03546
YER044C	YER044C	-0.76323	-0.995545	0.009447
YPL092W	YPL092W	-0.784119	-0.84839	0.077845
YML075C	YML075C	-0.66478	-0.742785	0.31812
YPL066W	YPL066W	-0.538909	-0.641721	0.178508
YMR030W-A	YMR030W	-0.616896	-0.454838	0.084452
YJL117W	YJL117W	-0.600328	-0.511951	0.060395
YMR032W	YMR032W	-0.641548	-0.584348	0.017399
YER056C	YER056C	-0.658738	-0.60332	-0.057556
YHR022C	YHR022C	-0.730672	-0.465317	0.488107
YNR009W	YNR009W	-0.639524	-0.539942	0.276325
YPL068C	YPL068C	-0.639863	-0.390321	0.311581
YDR044W	YDR044W	-0.787838	-0.718158	0.576189
YPL057C	YPL057C	-1.304416	-0.453506	-0.09573
YNL327W	YNL327W	-1.419537	-0.456658	-0.035435
YGR272C	YGR272C	-1.318424	-0.351872	-0.051133
YJR048W	YJR048W	-1.257396	-0.326339	0.014971
YOL019W	YOL019W	-1.288769	-0.387384	0.11906
YKL099C	YKL099C	-1.150759	-0.220279	0.07291
YHR066W	YHR066W	-1.304707	-0.185313	0.03815
YOR095C	YOR095C	-0.997563	-0.35532	0.050813
YAL059W	YAL059W	-0.994499	-0.398791	0.0139

YNL162W-A	YNL162W-	-1.05393	-0.314222	-0.022577
YIL158W	YIL158W	-1.038477	-0.298129	0.012811
YMR239C	YMR239C	-1.079968	-0.323804	0.015705
YDR184C	YDR184C	-1.117233	-0.405462	0.066926
YPL146C	YPL146C	-1.097313	-0.341373	0.089128
YLR073C	YLR073C	-1.124565	-0.367879	-0.154846
YHR052W	YHR052W	-1.096203	-0.388025	-0.038756
YMR015C	YMR015C	-1.192328	-0.529732	-0.121981
YEL040W	YEL040W	-1.140605	-0.537784	-0.084598
YNL024C	YNL024C	-1.124738	-0.668689	-0.176781
YOR072W-B	YOR072W-	-1.179767	-0.501843	-0.313012
YMR011W	YMR011W	-1.047188	-0.494915	-0.209743
YDL179W	YDL179W	-1.4164	-0.376551	-0.21954
YGR271C-A	YGR271C-A	-1.367881	-0.301543	-0.243718
YER124C	YER124C	-1.394713	-0.365854	-0.539364
YPL061W	YPL061W	-1.293322	-0.005912	-0.610692
YBL028C	YBL028C	-1.025202	-0.206871	-0.053283
YGL028C	YGL028C	-0.98148	-0.264637	-0.118008
YCR020W-B	YCR020W-	-1.018662	-0.087625	-0.049605
YJL011C	YJL011C	-0.792154	-0.010188	-0.011872
YPL158C	YPL158C	-0.814284	0.01076	-0.092527
YHR196W	YHR196W	-0.863989	-0.165838	-0.124069
YLR287C	YLR287C	-0.782722	-0.099197	-0.197116
YOL020W	YOL020W	-0.739805	-0.203711	-0.071481
YOR159C	YOR159C	-0.673594	-0.138845	-0.077676
YPL227C	YPL227C	-0.680673	-0.181158	-0.113845
YLR264W	YLR264W	-0.649254	-0.204616	-0.20628
YPL163C	YPL163C	-0.819237	-0.39144	-0.165403
YCR043C	YCR043C	-0.828681	-0.340857	-0.196241
YBL055C	YBL055C	-0.690262	-0.333605	-0.148308
YKL164C	YKL164C	-0.886037	-0.389714	-0.091537
YLR285C-A	YLR285C-A	-0.812289	-0.440132	-0.07874
YKR061W	YKR061W	-0.855789	-0.461683	0.016426
YNL075W	YNL075W	-0.873769	-0.303583	0.06103
YOR119C	YOR119C	-0.88207	-0.345121	0.01433
YOR004W	YOR004W	-0.878897	-0.356542	0.055945
YGR081C	YGR081C	-0.886528	-0.245544	-0.064313
YDL063C	YDL063C	-0.8893	-0.297907	-0.073846
YML043C	YML043C	-0.904041	-0.215257	-0.006759
YNL300W	YNL300W	-0.767885	-0.357339	0.057677
YPL165C	YPL165C	-0.804397	-0.320086	0.053357
YOL144W	YOL144W	-0.742002	-0.28505	0.092757
YML080W	YML080W	-0.808155	-0.343047	-0.05663
YNL034W	YNL034W	-0.798485	-0.305995	-0.046402
YNL119W	YNL119W	-0.738471	-0.290834	-0.06127
YDR399W	YDR399W	-0.730769	-0.433201	-0.034015
YDL042C	YDL042C	-0.852518	-0.28447	0.312551
YJL122W	YJL122W	-0.801952	-0.352235	0.287684
YGR041W	YGR041W	-0.81707	-0.416311	0.221974
YLR063W	YLR063W	-0.785169	-0.351531	0.189522

YHR169W	YHR169W	-0.921531	-0.335304	0.213397
YLR363W-A	YLR363W-	-0.940268	-0.214857	0.080432
YNL301C	YNL301C	-0.952251	-0.208943	0.084877
YDR299W	YDR299W	-0.920373	-0.242432	0.116508
YGL029W	YGL029W	-0.974169	-0.244291	0.044468
YHR197W	YHR197W	-0.983111	-0.326906	0.130451
YLL011W	YLL011W	-0.978058	-0.249897	0.129031
YNL182C	YNL182C	-1.00086	-0.256279	0.160956
YOR287C	YOR287C	-1.026403	-0.257126	0.214451
YOL080C	YOL080C	-1.069416	-0.271948	0.147793
YLR068W	YLR068W	-0.939414	-0.062827	0.087384
YOR342C	YOR342C	-0.809384	-0.059979	0.125933
YCR016W	YCR016W	-0.852698	-0.095476	0.052606
YOR264W	YOR264W	-0.85863	0.023682	0.160862
YDR412W	YDR412W	-0.840776	0.039301	0.100001
YPL245W	YPL245W	-0.926171	0.073276	0.256865
YIL019W	YIL019W	-0.824764	0.091556	0.273614
YDR083W	YDR083W	-0.915437	-0.173763	0.247534
YHR085W	YHR085W	-0.837462	-0.253564	0.215562
YDR324C	YDR324C	-0.829401	-0.198156	0.256622
YLR003C	YLR003C	-0.766628	-0.120755	0.136361
YGR187C	YGR187C	-0.740108	-0.130188	0.16448
YDR361C	YDR361C	-0.806214	-0.157068	0.185872
YPR137W	YPR137W	-0.771569	-0.095819	0.253034
YIL103W	YIL103W	-0.822611	-0.177048	-8.72E-04
YJL148W	YJL148W	-0.804848	-0.162139	0.02211
YDR449C	YDR449C	-0.828149	-0.23701	0.019955
YIL091C	YIL091C	-0.829529	-0.198132	0.05289
YER127W	YER127W	-0.877939	-0.199958	0.148394
YNL111C	YNL111C	-0.809315	-0.218915	0.120586
YKR024C	YKR024C	-0.780613	-0.240749	0.136802
YDL043C	YDL043C	-0.748002	-0.186336	0.044226
YGR283C	YGR283C	-0.78912	-0.186846	0.043388
YLR347C	YLR347C	-0.71737	-0.127022	0.065812
YLR222C	YLR222C	-0.762311	-0.144403	0.06022
YFL034C-A	YFL034C-A	-0.621965	-0.448212	-0.283375
YPR166C	YPR166C	-0.652454	-0.411842	-0.275068
YPR106W	YPR106W	-0.62125	-0.625154	-0.222107
YDR210W	YDR210W	-0.76796	-0.353979	-0.35536
YJL096W	YJL096W	-0.585856	-0.368384	-0.041313
YNL169C	YNL169C	-0.525778	-0.303254	-0.144911
YPR108W-A	YPR108W-	-0.549497	-0.331522	-0.176694
YDR070C	YDR070C	-0.790551	-0.667047	-0.574221
YMR118C	YMR118C	-0.573588	-0.551602	-0.631359
YML058W-A	YML058W-	-0.593191	0.265816	-0.440319
YML108W	YML108W	-0.495256	0.063711	-0.148922
YKL096W	YKL096W	-1.5604	-0.110821	0.363457
YMR230W-A	YMR230W	-1.686877	-0.517905	0.255474
YKL078W	YKL078W	-1.078741	-0.409123	0.246475
YDL241W	YDL241W	-1.03905	-0.521772	0.4537

YLR121C	YLR121C	-1.1101156	-0.093144	0.584482
YHR094C	YHR094C	-1.207275	0.243913	0.274392
YNR067C	YNR067C	-1.430648	0.257047	0.118234
YDR222W	YDR222W	-1.421418	0.408224	0.079002
YJR070C	YJR070C	-0.569932	-0.180888	0.142184
YLR409C	YLR409C	-0.618153	-0.238689	0.185317
YLR221C	YLR221C	-0.612013	-0.171469	0.213431
YOR340C	YOR340C	-0.615029	-0.141354	0.225569
YKL166C	YKL166C	-0.69773	-0.1267	0.148319
YJL069C	YJL069C	-0.678246	-0.180436	0.173403
YNL175C	YNL175C	-0.665957	-0.110683	0.207458
YLR099C	YLR099C	-0.403286	-0.129096	0.199719
YDR398W	YDR398W	-0.530144	-0.079465	0.183036
YPL069C	YPL069C	-0.607505	0.072517	0.178488
YOL007C	YOL007C	-0.626065	-0.02273	0.183157
YOR091W	YOR091W	-0.6291	-0.014712	0.163624
YPR143W	YPR143W	-0.62508	0.010663	0.175941
YDR087C	YDR087C	-0.654831	-0.003588	0.136556
YIL127C	YIL127C	-0.779948	-0.014545	0.186459
YDR021W	YDR021W	-0.740934	0.048523	0.200147
YER082C	YER082C	-0.706368	-0.012994	0.202725
YOL010W	YOL010W	-0.638388	0.015929	0.237123
YDR365C	YDR365C	-0.709428	0.021993	0.278121
YAL025C	YAL025C	-0.635748	-0.014059	0.325016
YIL104C	YIL104C	-0.628021	-0.131091	0.288274
YBR247C	YBR247C	-0.694492	-0.127991	0.286097
YPL043W	YPL043W	-0.696074	-0.090589	0.270935
YBR267W	YBR267W	-0.668156	-0.086142	0.323763
YBR271W	YBR271W	-0.561659	-0.021174	0.463252
YER028C	YER028C	-0.63341	0.196135	0.762258

Table S2: List of Group 1 AA genes

1810 = SWI2 Anchor away; 1854= SWI2 Anchor away sir3 null mutant; 1853 = sir3 null in Anchor away background; 1809 = Wildtype Anchor away background. _R = with Rapamycin

YORF	NAME	1810_R1-1809_R	1854_R1-1809_R	1853_R-1809_R
YLR154W-E	null	-1.555192	-0.351773	-1.73793
YHR137W	ARO9	-1.964415	-0.29048	-1.25603
YDL037C	BSC1	-2.301298	0.054224	-1.61956
YFR032C	RRT5	-2.357541	-1.169374	-1.62064
YDR380W	ARO10	-2.408232	-1.078401	-1.12321
YDR384C	ATO3	-2.591182	-1.606145	-1.25726
YJL012C	VTC4	-1.730655	-1.150325	-0.70305
YPL279C	FEX2	-1.909143	-0.916844	-0.62966
YOR390W	FEX1	-1.718305	-0.730397	-0.87149
YMR189W	GCV2	-1.884147	-0.76806	-0.89462
YJL047C-A	null	-1.877745	-0.735646	-1.1494
YNR044W	AGA1	-1.889627	-0.851457	-1.22788
YNL197C	WHI3	-2.013228	-0.787274	-1.16914
YLR342W-A	null	-2.13461	-1.120897	-0.62122
YGR041W	BUD9	-2.429062	-1.035065	-0.73259
YKL043W	PHD1	-2.449638	-1.059257	-0.481
YJR147W	HMS2	-2.521508	-0.68129	-0.66571
YKR050W	TRK2	-1.564904	-0.905273	-0.28193
YOR034C	AKR2	-1.47363	-0.878702	-0.31952
YLL066W-B	null	-1.63241	-0.823486	-0.21775
YGR233C	PHO81	-1.485611	-0.980128	-0.03703
YDL042C	SIR2	-1.420121	-0.998536	-0.09364
YKR104W	null	-1.229861	-0.567416	0.079281
YOR066W	MSA1	-1.373663	-0.658872	-0.06609
YFL021W	GAT1	-1.39381	-0.739817	0.070213
YOL020W	TAT2	-1.611607	-0.635395	-0.02211
YLR285C-A	null	-1.578821	-0.490248	0.013808
YBR296C	PHO89	-1.466358	-0.626254	0.239036
YGR143W	SKN1	-1.472033	-0.868274	0.301284
YBR196C-A	null	-1.686044	-1.024496	0.365435
YGR068C	ART5	-1.308685	-1.367768	-0.25619
YPR009W	SUT2	-1.199259	-1.578666	-0.1354
YPL066W	RGL1	-1.00754	-1.297962	-0.02652
YLR278C	null	-1.039162	-1.355646	0.097341
YBR291C	CTP1	-1.350511	-1.317544	0.568544
YBL042C	FUI1	-1.223819	-0.91923	0.308592
YOR342C	null	-1.000736	-1.138968	0.459689
YPR106W	ISR1	-1.79978	-0.483187	-0.2268
YOR084W	LPX1	-1.799683	-0.689908	-0.43065
YOR137C	SIA1	-1.75522	-0.752846	-0.40568
YIR019C	FLO11	-1.986636	-0.540304	-0.32771
YMR266W	RSN1	-2.049499	-0.570817	-0.53056
YDR072C	IPT1	-1.593271	0.019658	-0.28354
YNR067C	DSE4	-1.660394	-0.136176	-0.36397
YGL028C	SCW11	-1.830712	-0.060328	-0.32761

YLR139C	SLS1	-2.083937	-0.41219	0.129681
YOR383C	FIT3	-1.95521	-0.253077	0.131117
YMR011W	HXT2	-1.933943	-0.067735	0.024425
YGR249W	MGA1	-1.655524	-0.177218	0.18255
YDR038C	ENA5	-1.198654	-0.029782	-0.27106
YMR155W	null	-1.220131	-0.173316	-0.18325
YNL327W	EGT2	-1.412944	-0.034828	-0.17192
YDL195W	SEC31	-1.348284	-0.172596	-0.38395
YOL105C	WSC3	-1.292077	-0.338939	-0.38492
YAL021C	CCR4	-1.257148	-0.375177	-0.42389
YGL063W	PUS2	-1.154045	-0.379087	-0.23419
YOR081C	TGL5	-1.149228	-0.377802	-0.29463
YHR151C	MTC6	-1.186217	-0.269886	-0.29443
YCR048W	ARE1	-1.105687	-0.121713	-0.47338
YOR098C	NUP1	-1.068292	-0.063428	-0.44489
YOR149C	SMP3	-1.034922	-0.057169	-0.43783
YER154W	OXA1	-1.039944	-0.252443	-0.41311
YHR143W	DSE2	-1.102243	-0.245431	-0.38771
YEL017W	GTT3	-1.29664	-0.207355	-0.66235
YOL158C	ENB1	-1.43844	-0.320369	-0.77348
YOR068C	VAM10	-1.052164	-0.447297	-0.52555
YNL251C	NRD1	-1.223235	-0.360766	-0.62714
YBL004W	UTP20	-1.193647	-0.431908	-0.60151
YJL062W	LAS21	-1.224755	-0.486421	-0.66804
YOR160W	MTR10	-1.199381	-0.529148	-0.52078
YCR084C	TUP1	-1.191201	-0.64103	-0.54665
YHR042W	NCP1	-1.132657	-0.631171	-0.55374
YNL275W	BOR1	-1.148786	-0.62428	-0.55425
YJL198W	PHO90	-1.249746	-0.669753	-0.43839
YBL081W	null	-1.382356	-0.512508	-0.48926
YPL056C	LCL1	-1.305682	-0.50234	-0.49005
YLR397C	AFG2	-1.246947	-0.564002	-0.18438
YPL041C	null	-1.197879	-0.597596	-0.27577
YBR239C	ERT1	-1.151174	-0.694096	-0.13321
YMR310C	null	-1.088656	-0.7018	-0.10469
YNL278W	CAF120	-1.041454	-0.441577	-0.07463
YKR053C	YSR3	-1.066398	-0.578892	-0.05501
YAL037W	null	-1.007443	-0.678412	0.04718
YAR029W	null	-1.053898	-0.631209	0.287797
YGL162W	SUT1	-1.301283	-0.314407	-0.06362
YOR359W	VTS1	-1.213828	-0.250429	-0.0447
YOR161C	PNS1	-1.238826	-0.276779	-0.09367
YPL076W	GPI2	-1.312037	-0.184898	0.136374
YCL005W	LDB16	-1.081465	-0.277874	0.020287
YJL216C	IMA5	-1.05942	-0.269345	0.081337
YNL034W	null	-1.018354	-0.190546	-0.12339
YMR013C	SEC59	-1.08777	-0.242867	-0.1055
YNL288W	CAF40	-1.095138	-0.264427	-0.15225
YBL101W-B	null	-1.014151	-0.995121	-0.19002
YBR301W	PAU24	-1.260484	-0.925733	-0.24493

YNL204C	SPS18	-1.175955	-0.853385	-0.27685
YJL193W	null	-1.368008	-0.862954	-0.3361
YDR143C	SAN1	-1.293169	-0.8678	-0.39477
YPR054W	SMK1	-1.248613	-1.072935	-0.34598
YNL291C	MID1	-1.077109	-0.769886	-0.70305
YDR538W	PAD1	-1.040836	-0.710045	-0.72063
YLR459W	GAB1	-1.0176	-0.644804	-0.73487
YDR404C	RPB7	-1.108425	-0.793386	-0.61565
YHR163W	SOL3	-1.082184	-0.831005	-0.57453
YOL052C	SPE2	-1.04761	-0.873968	-0.6079
YPR121W	THI22	-1.021577	-0.693926	-0.36949
YHR086W-A	null	-1.059386	-0.784566	-0.40747
YNR055C	HOL1	-1.113354	-0.745037	-0.50927
YOR321W	PMT3	-1.080195	-0.7333	-0.57796
YKL078W	DHR2	-1.047444	-0.702301	-0.58379
YPL162C	null	-1.091111	-0.657734	-0.54618
YBR086C	IST2	-1.022796	-0.622193	-0.57988
YMR274C	RCE1	-1.413554	-0.919902	-0.55519
YCR065W	HCM1	-1.285848	-0.962969	-0.67737
YEL065W	SIT1	-1.326927	-0.783409	-0.60061
YHR086W	NAM8	-1.318066	-0.818393	-0.61668
YGR281W	YOR1	-1.281143	-0.81167	-0.52579
YDL179W	PCL9	-1.268798	-0.745332	-0.50394
YLR141W	RRN5	-1.303257	-0.781836	-0.77922
YGR038W	ORM1	-1.246203	-0.704735	-0.74587
YLL031C	GPI13	-1.30253	-0.643208	-0.68088
YBR175W	SWD3	-1.260419	-1.254828	-0.86015
YER110C	KAP123	-1.067729	-1.093829	-0.8948
YGR131W	FHN1	-1.038851	-1.171217	-0.9338
YBR074W	PFF1	-1.063322	-1.206995	-0.77965
YMR277W	FCP1	-1.041506	-0.97864	-0.84932
YPR052C	NHP6A	-1.022073	-0.965162	-0.68902
YLR380W	CSR1	-1.085019	-0.869708	-0.74981
YNL238W	KEX2	-1.107759	-0.93974	-0.74767
YPR128C	ANT1	-1.14267	-0.956547	-0.6306
YPL018W	CTF19	-1.096172	-0.982328	-0.61275
YCL002C	null	-1.095239	-1.116041	-0.62248
YOR129C	AFI1	-1.366272	-1.293772	-0.5899
YNL080C	EOS1	-1.293655	-1.163043	-0.53001
YOR378W	AMF1	-1.008824	-0.401119	-1.10451
YGR146C-A	null	-1.037179	-0.253796	-1.17931
YBL112C	null	-1.087553	-0.294808	-0.86761
YEL007W	MIT1	-1.450384	-0.175074	-1.11328
YBL032W	HEK2	-1.428298	-0.549564	-1.20662
YMR055C	BUB2	-1.32715	-0.832963	-0.8408
YDL093W	PMT5	-1.285507	-0.896378	-0.84831
YLR381W	CTF3	-1.309061	-0.870505	-0.88433
YNR060W	FRE4	-1.404624	-0.994241	-0.99664
YJR124C	null	-1.421199	-0.870187	-0.82313
YPL128C	TBF1	-1.46835	-0.971687	-0.79808

YML059C	NTE1	-1.559741	-0.877355	-0.76925
YDL160C	DHH1	-1.460546	-0.712223	-0.80449
YDR044W	HEM13	-1.482312	-0.685862	-0.96316
YDR414C	ERD1	-1.115155	-0.567869	-1.01918
YOR307C	SLY41	-1.176199	-0.6677	-0.94427
YEL042W	GDA1	-1.208786	-0.640769	-1.01143
YNL283C	WSC2	-1.176128	-0.87668	-0.95097
YOR067C	ALG8	-1.246612	-0.771258	-1.00481
YHR115C	DMA1	-1.122361	-0.725427	-0.90375
YDL048C	STP4	-1.213949	1.304484	1.386136
YCL068C	null	-1.523301	1.657408	1.603099
YFR022W	ROG3	-1.101124	1.820295	2.165995
YCR108C	null	-1.06561	1.33408	2.05838
YPL165C	SET6	-2.289622	1.097893	2.20319
YMR182C	RGM1	-1.899901	1.352962	1.640581
YDR247W	VHS1	-1.800171	1.391117	1.98415
YPL014W	null	-1.910601	1.698177	2.742215
YER028C	MIG3	-1.415682	1.989151	0.358269
YOL011W	PLB3	-1.942625	0.632071	1.215531
YER188C-A	null	-2.006381	0.225677	0.750596
YER088C	DOT6	-1.230253	0.578579	0.870996
YLR120C	YPS1	-1.208372	0.519998	0.838073
YBR298C	MAL31	-1.420194	0.582458	0.997994
YKL220C	FRE2	-1.163377	0.038322	0.585177
YOL136C	PFK27	-1.330024	0.122457	0.50754
YBL111C	null	-1.481711	0.309395	0.461409
YHL040C	ARN1	-1.378605	0.368258	0.793778
YEL063C	CAN1	-1.266327	0.260261	0.646736
YOR273C	TPO4	-1.594325	0.143492	0.763655
YDR534C	FIT1	-1.637009	0.208779	0.328522
YOR381W	FRE3	-1.59899	0.290977	0.265652
YCR089W	FIG2	-1.756856	0.166196	0.177603
YPL057C	SUR1	-1.782771	0.123331	0.541527
YAL040C	CLN3	-1.861156	0.015472	0.404578
YLR152C	null	-1.285577	-0.35867	0.317725
YAL060W	BDH1	-1.328006	-0.452297	0.269904
YBR021W	FUR4	-1.114172	-0.330952	0.547602
YKL029C	MAE1	-1.253982	-0.332381	0.555527
YMR272C	SCS7	-1.212712	-0.223203	0.405308
YOL059W	GPD2	-1.007211	-0.056624	0.831813
YGL256W	ADH4	-1.093417	-0.305503	0.710373
YLL066W-B	null	-1.952956	-0.33443	0.509491
YAR010C	null	-1.799371	-0.406109	0.645434
YHL016C	DUR3	-1.741483	-0.492125	0.35648
YBR196C-B	null	-1.369806	-0.58939	0.657573
YCL025C	AGP1	-1.682185	-0.331049	0.823672
YDR205W	MSC2	-1.001279	0.140402	-0.1044
YIL006W	YIA6	-1.039886	0.124122	-0.01684
YLR337C	VRP1	-1.096899	0.188038	-0.00914
YNL321W	VNX1	-1.180766	0.100233	-0.12292

YMR120C	ADE17	-1.211862	0.029671	-0.08318
YPL190C	NAB3	-1.246992	0.338697	-0.18057
YOR140W	SFL1	-1.290206	0.326112	-0.15347
YMR069W	NAT4	-1.221564	0.089779	0.273154
YKR102W	FLO10	-1.275704	0.194769	0.316539
YDR232W	HEM1	-1.332911	0.045818	0.348183
YDR246W-A	null	-1.440417	0.158604	0.091489
YDL140C	RPO21	-1.31474	0.154825	0.066087
YBR020W	GAL1	-1.311369	0.086624	0.107964
YOR349W	CIN1	-1.048967	-0.045259	0.035903
YAL020C	ATS1	-1.068134	-0.002847	0.125437
YGR079W	null	-1.15463	-0.053631	0.260586
YER152C	null	-1.022108	-0.125026	0.246497
YAL063C	FLO9	-1.067861	-0.071818	0.206601
YKL187C	FAT3	-1.036015	0.178003	0.196359
YLR116W	MSL5	-1.06763	0.179945	0.243781
YKL198C	PTK1	-1.096863	0.259249	0.20616
YDR160W	SSY1	-1.019812	0.148067	0.308233
YER060W	FCY21	-1.029224	0.203936	0.351275
YGL178W	MPT5	-1.179571	0.479767	0.359187
YDR438W	THI74	-1.258853	0.579677	0.370009
YLR099C	ICT1	-1.13923	0.600478	0.329931
YLR403W	SFP1	-1.212804	0.429344	0.237323
YJL094C	KHA1	-1.017959	0.514731	0.080093
YMR008C	PLB1	-1.103382	0.676622	0.553909
YGR289C	MAL11	-1.084481	0.696059	0.692787
YPL015C	HST2	-1.078514	1.148372	0.591381
YHR094C	HXT1	-1.578098	0.964523	0.494114
YGR023W	MTL1	-1.551499	0.762923	0.690967
YMR291W	TDA1	-1.2614	0.269249	1.804324
YGR032W	GSC2	-1.242827	0.236364	1.776908
YJL079C	PRY1	-1.443107	0.230725	1.836415
YBR067C	TIP1	-1.191979	0.6789	2.078076
YHL026C	null	-1.244398	0.708651	1.464342
YGR121C	MEP1	-1.02356	0.688905	1.588961
YER053C	PIC2	-1.617607	0.204335	1.427363
YJL212C	OPT1	-1.53264	0.103232	1.427167
YER158C	null	-1.423766	0.170882	1.213202
YPL036W	PMA2	-1.151877	-0.145902	1.544101
YLR142W	PUT1	-1.002157	0.184707	1.238826
YOR071C	NRT1	-1.17284	-0.074057	1.26817
YGR260W	TNA1	-1.147552	0.084828	1.242491
YFL014W	HSP12	-1.292276	0.237658	2.488439
YPL092W	SSU1	-1.065039	-0.681846	0.960938
YBL005W-A	null	-1.17081	-0.719291	0.961157
YNL024C	null	-1.26106	-0.90903	1.338866
YNR014W	null	-1.922514	-0.605679	1.777716
YPR160W	GPH1	-1.099576	-0.583531	2.009052
YOL104C	NDJ1	-1.647413	-1.534572	1.433746
YDR222W	null	-2.011217	-1.458479	0.856427

YCR018C	SRD1	-1.838414	-2.480437	1.389827
YHR033W	null	-1.916852	-1.503132	2.110011
YOL052C-A	DDR2	-1.365443	-0.876442	3.35148
YMR081C	ISF1	-1.715576	-1.687342	3.543186
YHR092C	HXT4	-3.350206	0.671244	0.82595
YDL039C	PRM7	-2.859618	0.584578	0.03101
YDL038C	null	-3.677256	0.345895	-0.19471
YBR238C	null	-2.643991	-0.768649	-0.05108
YLR466C-B	null	-2.556635	-0.702605	0.286957
YOR394C-A	null	-2.463799	-0.091134	0.527107
YLR466C-B	null	-2.4757	-0.355529	0.395135
YLL066W-B	null	-2.254415	-0.214519	0.728592
YJL078C	PRY3	-2.463906	0.045136	0.17965
YDR342C	HXT7	-2.174849	-0.87236	1.142651
YER067W	RGI1	-2.320877	-1.049696	1.041793
YOR092W	ECM3	-2.179419	-0.617264	0.945413
YLR121C	YPS3	-2.161079	-0.657103	0.534248
YCR097W	HMRA1	-5.067512	-0.8165	0.728803

Table S3: List of Group 1 genes common in the KO and AA datasets

swi2D = swi2 null mutant; swi2Dsir3D= swi2 and sir3 null mutant, sir3D = sir3 null mutant, WT = Wildtype, 1810 = SWI2 Anchor away; 1854= SWI2 Anchor away sir3 null mutant; 1853 = sir3 null in Anchor away background; 1809 = Wildtype Anchor away background. _R = with Rapamycin

YORF	NAME	swi2D-WT	swi2Dsir3D-WT	sir3D-WT	1810_R1-1809_R	1854_R1-1809_R	1853_R-1809_R
YBR238C	YBR238(	-1.113228	-1.032084	0.050758	-2.643991	-0.768649	-0.051082
YER028C	MIG3	-0.63341	0.196135	0.762258	-1.415682	1.989151	0.358269
YHR094C	HXT1	-1.207275	0.243913	0.274392	-1.578098	0.964523	0.494114
YKL078W	DHR2	-1.078741	-0.409123	0.246475	-1.047444	-0.702301	-0.583786
YDL042C	SIR2	-0.852518	-0.28447	0.312551	-1.420121	-0.998536	-0.093641
YDL179W	PCL9	-1.4164	-0.376551	-0.21954	-1.268798	-0.745332	-0.503944
YDR044W	HEM13	-0.787838	-0.718158	0.576189	-1.482312	-0.685862	-0.96316
YDR222W	YDR222	-1.421418	0.408224	0.079002	-2.011217	-1.458479	0.856427
YDR384C	ATO3	-0.95195	-0.607941	0.163866	-2.591182	-1.606145	-1.25726
YGL028C	SCW11	-0.98148	-0.264637	-0.118008	-1.830712	-0.060328	-0.327612
YGR041W	BUD9	-0.81707	-0.416311	0.221974	-2.429062	-1.035065	-0.732587
YGR079W	YGR079	-1.056979	-0.935159	0.135865	-1.15463	-0.053631	0.260586
YLR099C	ICT1	-0.403286	-0.129096	0.199719	-1.13923	0.600478	0.329931
YLR121C	YPS3	-1.101156	-0.093144	0.564482	-2.161079	-0.657103	0.534248
YMR011W	HXT2	-1.047188	-0.494915	-0.209743	-1.933943	-0.067735	0.024425
YNL024C	EFM6	-1.124738	-0.668689	-0.176781	-1.26106	-0.90903	1.338866
YNL034W	YNL034	-0.798485	-0.305995	-0.046402	-1.018354	-0.190546	-0.123394
YNL327W	EGT2	-1.419537	-0.456658	-0.035435	-1.412944	-0.034828	-0.171923
YNR067C	DSE4	-1.430648	0.257047	0.118234	-1.660394	-0.136176	-0.363971
YOL020W	TAT2	-0.739805	-0.203711	-0.071481	-1.611607	-0.635395	-0.022112
YOR342C	YOR342	-0.809384	-0.059979	0.125933	-1.000736	-1.138968	0.459689
YPL057C	SUR1	-1.304416	-0.453506	-0.09573	-1.782771	0.123331	0.541527
YPL066W	RGL1	-0.538909	-0.641721	0.178508	-1.00754	-1.297962	-0.026519
YPL092W	SSU1	-0.784119	-0.84839	0.077845	-1.065039	-0.681846	0.960938
YPL165C	SET6	-0.804397	-0.320086	0.053357	-2.289622	1.097893	2.20319
YPR054W	SMK1	-0.786343	-0.572491	0.119735	-1.248613	-1.072935	-0.345981
YPR106W	ISR1	-0.62125	-0.625154	-0.222107	-1.79978	-0.483187	-0.226804
YLR285C-A	YLR285(	-0.812289	-0.440132	-0.07874	-1.578821	-0.490248	0.013808

Table S4: List of Group 2 KO genes

swi2D = swi2 null mutant; sir3D = sir3 null mutant, WT = Wildtype

YORF	NAME	swi2D-WT	swi2Dsir3D-WT	sir3D-WT
YHL012W	YHL012W	1.39651	0.363307	-0.024821
YDL170W	YDL170W	1.434712	0.331249	0.178301
YLL060C	YLL060C	1.345331	0.409135	0.188886
YOL119C	YOL119C	1.472612	0.061144	-0.026633
YJR130C	YJR130C	1.328341	0.18232	0.025941
YAL028W	YAL028W	1.252044	0.133739	-0.110437
YER175C	YER175C	1.426577	-0.142406	0.086255
YNL270C	YNL270C	1.526947	-0.30727	-0.022384
YBR145W	YBR145W	1.176709	-0.413801	0.091954
YOR289W	YOR289W	1.303741	0.188904	-0.363791
YJL089W	YJL089W	1.392584	0.290784	-0.29782
YIL037C	YIL037C	1.46089	0.263056	-0.534638
YNL194C	YNL194C	1.510503	0.334908	-0.37898
YCL040W	YCL040W	1.474825	0.407789	-0.438249
YKR076W	YKR076W	1.346451	0.424563	-0.370127
YDR516C	YDR516C	1.157875	0.424397	-0.411819
YHL044W	YHL044W	1.284105	0.442617	-0.568168
YDR309C	YDR309C	1.169489	0.019513	-0.596586
YGL032C	YGL032C	1.138942	-0.080326	-0.509035
YDL085W	YDL085W	1.278246	-0.204536	-0.537333
YJL103C	YJL103C	1.095172	0.228025	-0.301721
YMR306W	YMR306W	1.062371	0.272699	-0.358249
YOL083W	YOL083W	1.006853	0.361934	-0.320293
YLR270W	YLR270W	0.941675	0.318399	-0.313685
YAR023C	YAR023C	0.861997	0.295574	-0.298766
YKL142W	YKL142W	0.833649	0.292383	-0.429116
YGL104C	YGL104C	0.867143	0.316828	-0.374073
YAR068W	YAR068W	0.80976	-0.118429	-0.470585
YDL090C	YDL090C	0.790183	-0.041284	-0.312308
YHL022C	YHL022C	0.888585	0.242201	-0.507559
YKL217W	YKL217W	0.882017	0.095171	-0.621602
YGL185C	YGL185C	0.946109	0.881844	-0.050654
YKR066C	YKR066C	1.025034	0.91132	-0.026599
YJR103W	YJR103W	1.067124	0.916631	-0.012947
YPL134C	YPL134C	1.014002	0.862032	0.00447
YLR142W	YLR142W	1.010006	0.816799	0.045308
YCR037C	YCR037C	1.023084	0.81118	0.038704
YEL044W	YEL044W	0.991116	0.832672	0.08014
YGL183C	YGL183C	0.952034	0.767311	-0.026404
YBR230C	YBR230C	0.892935	0.76316	-0.091499
YLR412C-A	YLR412C-A	0.890019	0.81298	-0.054856
YGL081W	YGL081W	1.136778	0.526974	0.151449
YJL155C	YJL155C	1.155024	0.552499	0.052828
YLR356W	YLR356W	1.129004	0.560602	0.108706
YJL071W	YJL071W	1.092489	0.56018	0.082162
YMR094W	YMR094W	1.160889	0.638316	0.075412

YJL077W-A	YJL077W-A	1.141737	0.670945	0.127949
YKL086W	YKL086W	1.142035	0.673786	0.124597
YOL084W	YOL084W	1.132696	0.61427	0.148361
YDL149W	YDL149W	1.185467	0.659495	0.306894
YIL024C	YIL024C	1.11742	0.627506	0.220307
YPR036W-A	YPR036W-A	1.066355	0.731882	0.263468
YML120C	YML120C	1.088666	0.762926	0.128583
YDL138W	YDL138W	1.110095	0.72298	0.164833
YJR036C	YJR036C	1.178944	0.7529	0.138457
YPL113C	YPL113C	1.171352	0.720667	0.114903
YIL074C	YIL074C	1.244388	0.77317	0.168305
YML087C	YML087C	1.237079	0.686985	0.169487
YDR452W	YDR452W	0.886152	0.55767	0.04458
YIL046W	YIL046W	0.837093	0.584252	0.002653
YLR417W	YLR417W	0.825852	0.557197	0.027376
YLR350W	YLR350W	0.907203	0.641615	0.020785
YNR058W	YNR058W	0.886758	0.633461	0.005521
YBR150C	YBR150C	0.91409	0.524	0.02349
YGL036W	YGL036W	0.890575	0.485573	0.015498
YOR177C	YOR177C	0.893837	0.500689	-0.037962
YPR026W	YPR026W	0.87614	0.456565	-0.018907
YKL171W	YKL171W	0.837674	0.501156	0.094123
YKL026C	YKL026C	0.822128	0.459803	0.057352
YDL024C	YDL024C	0.793465	0.483795	-0.02712
YLR189C	YLR189C	0.775608	0.501842	-0.030236
YBR001C	YBR001C	0.819745	0.525976	-0.060255
YIL162W	YIL162W	0.813445	0.503346	0.017028
YDR022C	YDR022C	0.835347	0.516279	-0.019088
YKL107W	YKL107W	0.776387	0.59272	-0.069764
YMR020W	YMR020W	0.7955	0.546233	0.005497
YMR147W	YMR147W	0.761638	0.569792	-0.019936
YMR139W	YMR139W	0.708373	0.514123	0.018162
YGR207C	YGR207C	0.709674	0.545402	0.024355
YGR080W	YGR080W	0.6698	0.580932	0.029934
YOL032W	YOL032W	0.740201	0.607051	0.018664
YGL045W	YGL045W	0.74862	0.520836	0.126003
YMR114C	YMR114C	0.715137	0.581373	0.100723
YAL061W	YAL061W	1.080048	0.63144	0.015344
YFL042C	YFL042C	1.070022	0.600394	-0.016275
YHL024W	YHL024W	1.045911	0.667195	-0.027581
YKR097W	YKR097W	0.943387	0.652423	-0.043934
YDL027C	YDL027C	0.97885	0.647415	-0.060379
YJL045W	YJL045W	0.959893	0.616837	0.002423
YML100W	YML100W	1.017937	0.622644	0.003245
YGR250C	YGR250C	0.936389	0.749598	0.111166
YFL064C	YFL064C	0.931082	0.740061	0.099967
YPR155C	YPR155C	0.965036	0.741548	0.192373
YDR132C	YDR132C	0.969367	0.754427	0.131802
YMR030W	YMR030W	0.944327	0.78541	0.146986
YDR358W	YDR358W	1.018333	0.653511	0.189238

YMR302C	YMR302C	0.978898	0.661354	0.126652
YDL238C	YDL238C	0.978366	0.649432	0.148495
YKL129C	YKL129C	1.025219	0.573397	0.178255
YIR014W	YIR014W	1.018121	0.564928	0.195361
YNL077W	YNL077W	0.979824	0.611458	0.135164
YCR107W	YCR107W	0.94217	0.59097	0.159194
YLR260W	YLR260W	0.900669	0.607359	0.200363
YNR007C	YNR007C	0.953163	0.570762	0.235159
YBR285W	YBR285W	0.94172	0.618527	0.232708
YJL070C	YJL070C	0.960937	0.508825	0.348488
YOR113W	YOR113W	0.963024	0.536857	0.371851
YCR107W	YCR107W	1.011328	0.560049	0.300429
YIL107C	YIL107C	0.893802	0.522698	0.217952
YDL174C	YDL174C	0.913486	0.478663	0.255499
YFR047C	YFR047C	0.872582	0.528302	0.138168
YGR097W	YGR097W	0.88382	0.501875	0.141175
YIR031C	YIR031C	0.803063	0.515764	0.190921
YOR208W	YOR208W	0.86384	0.540229	0.311201
YKL124W	YKL124W	0.784504	0.516351	0.303699
YDR350C	YDR350C	0.799453	0.528983	0.306911
YIR007W	YIR007W	0.822092	0.502518	0.274489
YNL074C	YNL074C	0.917302	0.425195	0.170422
YMR160W	YMR160W	0.867979	0.440628	0.187692
YPR081C	YPR081C	0.879047	0.386579	0.248651
YEL072W	YEL072W	0.900306	0.35021	0.233605
YFL016C	YFL016C	0.913885	0.355887	0.209021
YIL154C	YIL154C	0.879745	0.374802	0.194374
YNL092W	YNL092W	0.800537	0.395907	0.117566
YGR239C	YGR239C	0.806245	0.398141	0.114831
YDL054C	YDL054C	0.844388	0.377671	0.146408
YNL223W	YNL223W	0.871289	0.349675	0.122003
YGL141W	YGL141W	0.782891	0.383586	0.187871
YEL059C-A	YEL059C-A	0.764673	0.385062	0.215634
YAR050W	YAR050W	0.78565	0.338906	0.218081
YCR063W	YCR063W	0.764622	0.39164	0.250625
YMR108W	YMR108W	0.831192	0.399722	0.26184
YJR091C	YJR091C	0.821343	0.399253	0.272638
YLR128W	YLR128W	0.819945	0.363568	0.275342
YOL036W	YOL036W	0.779427	0.430364	0.324494
YGR112W	YGR112W	0.779069	0.360068	0.323016
YBR241C	YBR241C	1.286382	0.394891	-0.056671
YBR169C	YBR169C	1.204758	0.444963	-0.070752
YIL072W	YIL072W	1.174991	0.353256	-0.188291
YOR100C	YOR100C	1.223167	0.34738	-0.226438
YJR025C	YJR025C	1.203687	0.27778	-0.095241
YKL151C	YKL151C	1.120125	0.47562	-0.130729
YOR386W	YOR386W	1.068739	0.405265	-0.187585
YGL227W	YGL227W	1.017435	0.512009	-0.119218
YKL023W	YKL023W	1.015047	0.484131	-0.127903
YJL037W	YJL037W	1.139261	0.529247	-0.300059

YOL048C	YOL048C	1.139063	0.575258	-0.303886
YNL012W	YNL012W	1.110718	0.658171	-0.298804
YLL058W	YLL058W	0.949158	0.342221	0.001809
YOR184W	YOR184W	0.946694	0.368402	0.076355
YLL023C	YLL023C	0.983143	0.256031	0.094348
YJL130C	YJL130C	0.868661	0.304314	0.075724
YOR215C	YOR215C	0.89009	0.302397	0.050161
YDR423C	YDR423C	0.903416	0.282427	0.096083
YOR226C	YOR226C	0.842657	0.289175	0.068865
YNL269W	YNL269W	0.848042	0.263558	0.07232
YIR018C-A	YIR018C-A	1.025414	0.177856	-0.012508
YMR271C	YMR271C	0.99798	0.221668	0.005056
YDR391C	YDR391C	1.041299	0.312647	-0.132675
YJL105W	YJL105W	1.085328	0.280285	-0.156777
YPR035W	YPR035W	1.053174	0.535779	0.147424
YMR181C	YMR181C	1.027823	0.499305	0.125681
YAR042W	YAR042W	0.996051	0.542491	0.106776
YBR256C	YBR256C	1.117128	0.472195	0.091479
YCR007C	YCR007C	1.094305	0.425895	0.114148
YJR151C	YJR151C	1.082374	0.41134	0.09249
YER039C-A	YER039C-A	1.08904	0.473621	-0.004792
YKR067W	YKR067W	0.943102	0.467276	0.025276
YDR085C	YDR085C	0.973096	0.461217	0.056368
YER061C	YER061C	0.982267	0.489825	0.011709
YLR345W	YLR345W	0.972745	0.481767	0.022308
YPR006C	YPR006C	0.959449	0.432701	-0.016602
YML042W	YML042W	1.01768	0.517468	-0.02032
YHL021C	YHL021C	1.001598	0.541008	0.028181
YKR101W	YKR101W	0.956901	0.530851	-0.036077
YDR255C	YDR255C	0.912978	0.261243	-0.111578
YBL029C-A	YBL029C-A	0.933231	0.294927	-0.143601
YKL091C	YKL091C	0.855291	0.27978	-0.159633
YOR044W	YOR044W	0.87909	0.311355	-0.12647
YGL208W	YGL208W	0.859363	0.358921	-0.064713
YMR042W	YMR042W	0.898176	0.375299	-0.051638
YHR016C	YHR016C	0.879494	0.393923	0.027684
YBR126C	YBR126C	0.864229	0.411888	0.005146
YPL123C	YPL123C	0.91806	0.410809	-0.13847
YNR002C	YNR002C	0.916208	0.41625	-0.169243
YKR011C	YKR011C	0.786404	0.457169	-0.211281
YOL110W	YOL110W	0.80485	0.465872	-0.178732
YAR027W	YAR027W	0.804986	0.46639	-0.104514
YBR046C	YBR046C	0.76371	0.400155	-0.129615
YER092W	YER092W	1.162289	0.800751	-0.290729
YOR220W	YOR220W	0.983114	0.816167	-0.289158
YOR052C	YOR052C	0.986094	0.772754	-0.547507
YLR151C	YLR151C	1.001377	0.662104	-0.488722
YGR087C	YGR087C	0.857261	0.827328	-0.421386
YBR070C	YBR070C	0.83713	0.799508	-0.493406
YLL039C	YLL039C	0.99209	0.547101	-0.323813

YDL130W	YDL130W	0.907984	0.601162	-0.38522
YBL064C	YBL064C	0.800049	0.467329	-0.319136
YJL060W	YJL060W	0.940977	0.632725	-0.183252
YPL060W	YPL060W	0.812251	0.65697	-0.276977
YOL117W	YOL117W	0.857969	0.727202	-0.14425
YBL106C	YBL106C	0.786351	0.744866	-0.141863
YER091C	YER091C	0.912795	0.791988	-0.20597
YLR273C	YLR273C	0.872978	0.781666	-0.179545
YNL191W	YNL191W	0.680276	0.768241	-0.040657
YFL065C	YFL065C	0.731623	0.810696	-0.096454
YER065C	YER065C	0.607262	0.831456	-0.076259
YMR226C	YMR226C	0.693075	0.562549	-0.138461
YEL070W	YEL070W	0.693348	0.537659	-0.214346
YKL067W	YKL067W	0.653262	0.623964	-0.271412
YBR077C	YBR077C	0.710257	0.661994	-0.187309
YLR364W	YLR364W	0.711243	0.632295	-0.214707
YPL188W	YPL188W	1.044743	0.437864	0.236191
YJR155W	YJR155W	1.021447	0.351439	0.127644
YDR254W	YDR254W	1.016065	0.420913	0.086022
YHR029C	YHR029C	1.195355	0.364526	0.140055
YOR389W	YOR389W	1.204943	0.247859	0.146578
YDL199C	YDL199C	1.135628	0.293484	0.222706
YPL278C	YPL278C	1.026999	0.235777	0.312092
YIL017C	YIL017C	0.984826	0.31048	0.32888
YMR062C	YMR062C	1.1203	0.253631	0.355844
YNR069C	YNR069C	1.094711	0.311196	0.40548
YEL049W	YEL049W	1.053544	0.16471	0.219588
YER044C-A	YER044C-A	1.023623	0.205459	0.176882
YOR178C	YOR178C	1.053549	0.09843	0.188446
YIL165C	YIL165C	1.024937	0.027316	0.082942
YJR109C	YJR109C	0.896324	0.057567	0.217495
YOR302W	YOR302W	0.892851	0.047607	0.149472
YPL272C	YPL272C	0.859388	0.109163	0.159569
YPR138C	YPR138C	1.183138	0.212706	0.294207
YOL058W	YOL058W	1.280412	0.119519	0.415834
YKL029C	YKL029C	0.836603	0.138751	0.607009
YLR348C	YLR348C	0.926576	0.168163	0.540016
YBR208C	YBR208C	0.999836	0.056315	0.435701
YOR192C	YOR192C	0.621194	-0.041284	0.296815
YGL006W	YGL006W	0.565981	0.022014	0.183108
YLL019C	YLL019C	0.657986	0.074146	0.40399
YJR127C	YJR127C	0.533803	0.132265	0.454976
YIL146C	YIL146C	0.526615	0.184867	0.459456
YOL064C	YOL064C	0.839878	0.210475	0.143075
YJL066C	YJL066C	0.870088	0.238017	0.138687
YOR303W	YOR303W	0.801709	0.241372	0.175243
YER185W	YER185W	0.824173	0.31181	0.168859
YLR299W	YLR299W	0.874008	0.283532	0.251899
YIL077C	YIL077C	0.917482	0.296003	0.252982
YPL264C	YPL264C	0.912513	0.193364	0.340127

YML002W	YML002W	0.789347	0.149882	0.186677
YLL029W	YLL029W	0.77421	0.195243	0.159444
YKR096W	YKR096W	0.656887	0.210722	0.242554
YPR174C	YPR174C	0.70807	0.202562	0.267917
YIR018W	YIR018W	0.719975	0.256673	0.267191
YJR154W	YJR154W	0.722351	0.278604	0.227509
YDR523C	YDR523C	0.797083	0.204144	0.372761
YDR035W	YDR035W	0.735675	0.111872	0.33354
YOR130C	YOR130C	0.78033	0.169009	0.272508
YCL039W	YCL039W	0.661805	0.356162	0.207619
YLL027W	YLL027W	0.66403	0.356883	0.224112
YMR301C	YMR301C	0.64884	0.401661	0.218619
YNL294C	YNL294C	0.66536	0.381563	0.177986
YLR425W	YLR425W	0.686342	0.353684	0.175994
YBR225W	YBR225W	0.753339	0.334112	0.163004
YOL154W	YOL154W	0.745044	0.360721	0.117354
YER040W	YER040W	0.660331	0.340628	0.135745
YDR313C	YDR313C	0.639926	0.344491	0.151312
YKR021W	YKR021W	0.650662	0.299474	0.115122
YNL116W	YNL116W	0.762514	0.47883	0.206979
YJR039W	YJR039W	0.750803	0.441322	0.218283
YER015W	YER015W	0.74053	0.479782	0.234071
YPR030W	YPR030W	0.731436	0.464757	0.250691
YHR082C	YHR082C	0.63274	0.428317	0.236665
YKR031C	YKR031C	0.633397	0.454192	0.241084
YDR475C	YDR475C	0.650787	0.486694	0.241377
YDR104C	YDR104C	0.666525	0.483899	0.227601
YPR168W	YPR168W	0.696583	0.420239	0.260633
YOL025W	YOL025W	0.652922	0.517804	0.098983
YDL178W	YDL178W	0.671546	0.537693	0.137707
YOR162C	YOR162C	0.673589	0.486348	0.173413
YGR237C	YGR237C	0.645323	0.479006	0.131874
YDR186C	YDR186C	0.659073	0.497597	0.1336
YOL164W	YOL164W	0.654549	0.493407	0.117831
YHR164C	YHR164C	0.576924	0.511361	0.156824
YDR169C	YDR169C	0.608993	0.501001	0.184884
YGL128C	YGL128C	0.518991	0.530357	0.255057
YJR052W	YJR052W	0.484051	0.507044	0.273634
YER047C	YER047C	0.577355	0.426424	0.302335
YBL084C	YBL084C	0.595973	0.480302	0.31422
YDL139C	YDL139C	0.595708	0.474896	0.275465
YCR100C	YCR100C	0.54992	0.484618	0.257613
YJR019C	YJR019C	0.572061	0.445319	0.206572
YOL091W	YOL091W	0.59534	0.255557	0.270565
YMR265C	YMR265C	0.567459	0.258728	0.23161
YGR126W	YGR126W	0.56534	0.251681	0.214237
YAL034C	YAL034C	0.564298	0.300951	0.280107
YPL164C	YPL164C	0.550972	0.345139	0.258162
YGR113W	YGR113W	0.479245	0.226193	0.277653
YMR135C	YMR135C	0.951011	0.352034	0.415563

YDR541C	YDR541C	0.884803	0.463204	0.555231
YKR102W	YKR102W	0.595357	0.284468	0.591786
YOR018W	YOR018W	0.764406	0.480334	0.561306
YJL100W	YJL100W	0.742634	0.433836	0.584511
YNL144C	YNL144C	0.705902	0.423877	0.493434
YFR022W	YFR022W	0.740657	0.402394	0.410533
YOR077W	YOR077W	0.690867	0.390151	0.388449
YNR065C	YNR065C	0.72087	0.386812	0.325778
YER162C	YER162C	0.733909	0.434537	0.323612
YOL051W	YOL051W	0.724742	0.441366	0.335819
YML076C	YML076C	0.670445	0.41375	0.322985
YGR258C	YGR258C	0.691146	0.408519	0.334469
YPR002W	YPR002W	0.67846	0.467907	0.362775
YCR024C	YCR024C	0.612769	0.360917	0.316836
YDR528W	YDR528W	0.580712	0.358707	0.381767
YMR253C	YMR253C	0.707862	0.277376	0.436816
YGR288W	YGR288W	0.680275	0.315446	0.372509
YGL219C	YGL219C	0.72029	0.280519	0.332057
YLL063C	YLL063C	0.737355	0.305061	0.310217
YMR182C	YMR182C	0.56691	-0.092589	0.650821
YJL161W	YJL161W	1.112427	-0.098702	-0.090355
YHR018C	YHR018C	1.097463	-0.010042	-0.282741
YBR214W	YBR214W	1.048822	0.08978	-0.19885
YLL055W	YLL055W	1.084256	0.034793	-0.084343
YGR019W	YGR019W	0.756911	0.03545	-0.17009
YJL163C	YJL163C	0.742659	-0.065623	-0.098911
YBR298C	YBR298C	0.965357	0.020371	-0.242704
YER096W	YER096W	0.903116	0.096143	-0.207056
YAR066W	YAR066W	0.867582	0.02989	-0.215754
YIL116W	YIL116W	0.845978	-0.160288	-0.082352
YMR018W	YMR018W	0.907539	-0.153467	0.050713
YBR183W	YBR183W	0.926466	-0.15967	-0.026584
YBR132C	YBR132C	0.956762	-0.269158	0.184922
YBR047W	YBR047W	0.916639	-0.148777	0.278189
YNL104C	YNL104C	0.777248	-0.15216	0.191172
YGR053C	YGR053C	0.752639	-0.138203	0.106464
YLR177W	YLR177W	0.904206	-0.048365	0.145183
YML116W	YML116W	0.857739	-0.136079	0.139293
YIR019C	YIR019C	0.647143	-0.018034	0.106158
YOR316C	YOR316C	0.663918	-0.065329	0.16934
YHL006C	YHL006C	0.724924	-0.028565	0.128995
YOR032W	YOR032W	0.585149	-0.072346	0.074312
YAL002W	YAL002W	0.593642	-0.046103	0.105006
YDR127W	YDR127W	0.676811	-0.068427	0.026518
YIL164C	YIL164C	0.686601	-0.036841	-0.011433
YER066W	YER066W	0.701785	0.018448	-0.028866
YML117W	YML117W	0.727407	-0.018494	-0.034254
YMR251W	YMR251W	0.684227	-0.14025	-0.001341
YGR070W	YGR070W	0.628337	-0.222661	0.002256
YGR045C	YGR045C	0.605165	-0.19431	-0.00647

YPL006W	YPL006W	0.586025	-0.036993	-0.038981
YIL088C	YIL088C	0.576831	-0.052844	-0.022622
YBR233W	YBR233W	0.628194	-0.054141	-0.004612
YOR173W	YOR173W	0.635113	-0.081923	-0.048003
YDR270W	YDR270W	0.535447	-0.175195	-0.006447
YOR081C	YOR081C	0.621488	-0.1019	-0.15413
YLR034C	YLR034C	0.557415	-0.117486	-0.134807
YAL017W	YAL017W	0.644572	-0.083116	-0.284143
YKR049C	YKR049C	0.659206	-0.169805	-0.259712
YPL257W	YPL257W	0.575563	-0.290897	-0.237339
YNR001C	YNR001C	0.835871	0.09965	0.025909
YDR479C	YDR479C	0.758988	0.148139	0.093184
YOL140W	YOL140W	0.769097	0.161215	0.067367
YCR069W	YCR069W	0.648985	0.061656	0.026119
YAL031C	YAL031C	0.671957	0.06073	0.013513
YHR198C	YHR198C	0.679071	0.140465	0.051539
YBR128C	YBR128C	0.649162	0.136315	0.071388
YMR053C	YMR053C	0.828506	0.206417	-0.09831
YDL216C	YDL216C	0.785739	0.188184	-0.049739
YMR019W	YMR019W	0.705654	0.105397	-0.030237
YLL041C	YLL041C	0.704188	0.090088	-0.102415
YHR006W	YHR006W	0.694044	0.384871	0.078626
YBR035C	YBR035C	0.681442	0.411983	0.066884
YDR436W	YDR436W	0.701215	0.499668	0.089
YPL230W	YPL230W	0.694019	0.486134	0.086743
YOR350C	YOR350C	0.697096	0.460254	0.072359
YMR278W	YMR278W	0.706045	0.401434	0.02805
YOR059C	YOR059C	0.727356	0.41682	0.015696
YDL035C	YDL035C	0.689415	0.387173	-0.040217
YJL141C	YJL141C	0.717176	0.374218	-0.028346
YIL097W	YIL097W	0.761334	0.428919	-0.055043
YPL109C	YPL109C	0.745653	0.426795	-0.017391
YKL065C	YKL065C	0.728626	0.478298	-0.019887
YAR028W	YAR028W	0.729349	0.465076	-0.023449
YDR191W	YDR191W	0.711605	0.465276	-0.022777
YFL041W-A	YFL041W-A	0.733267	0.457053	0.019081
YEL012W	YEL012W	0.766935	0.357536	0.046376
YJL048C	YJL048C	0.791764	0.395257	0.030323
YLR312C-B	YLR312C-B	0.771005	0.377709	0.00474
YGL181W	YGL181W	0.632044	0.475256	0.060042
YKL094W	YKL094W	0.573746	0.498888	0.024055
YNL014W	YNL014W	0.601777	0.477578	0.027808
YOR152C	YOR152C	0.611727	0.499225	0.013987
YKL104C	YKL104C	0.573801	0.358568	0.101818
YPL174C	YPL174C	0.603308	0.361553	0.106251
YCR026C	YCR026C	0.590847	0.387899	0.081455
YLR257W	YLR257W	0.582456	0.375314	0.091129
YDR383C	YDR383C	0.591796	0.444481	0.14362
YNL242W	YNL242W	0.624529	0.410285	0.114073
YDR058C	YDR058C	0.699754	0.509971	-0.07543

YAL053W	YAL053W	0.622956	0.309783	-0.07692
YNL115C	YNL115C	0.694435	0.42947	-0.072768
YMR009W	YMR009W	0.703049	0.430003	-0.061247
YKL045W	YKL045W	0.66072	0.453875	-0.025141
YLR456W	YLR456W	0.646774	0.458811	-0.03463
YDR178W	YDR178W	0.647255	0.39088	-0.080971
YMR110C	YMR110C	0.637669	0.429177	-0.121809
YOR022C	YOR022C	0.632565	0.471404	-0.130392
YER035W	YER035W	0.578698	0.416929	-0.014538
YIL007C	YIL007C	0.540788	0.426193	0.003844
YLR247C	YLR247C	0.542112	0.436357	-0.031952
YBR240C	YBR240C	0.561361	0.363311	-0.085969
YGR204W	YGR204W	0.69323	0.211582	-0.009774
YLR011W	YLR011W	0.668982	0.262527	0.00965
YOR202W	YOR202W	0.717327	0.198494	0.044077
YGL215W	YGL215W	0.671668	0.205455	0.070118
YBL015W	YBL015W	0.747799	0.276321	0.069803
YEL076C-A	YEL076C-A	0.770045	0.217755	0.05276
YLR001C	YLR001C	0.66106	0.324275	-0.010485
YKL211C	YKL211C	0.660756	0.314131	-0.025448
YKL157W	YKL157W	0.663763	0.296229	-0.046085
YPL166W	YPL166W	0.648425	0.321458	-0.057896
YFL010C	YFL010C	0.682652	0.336264	-0.06877
YDL234C	YDL234C	0.641924	0.369688	0.014474
YKL133C	YKL133C	0.633144	0.334711	0.001511
YBR248C	YBR248C	0.701947	0.337698	0.013052
YPL191C	YPL191C	0.735005	0.318631	-0.033382
YNL241C	YNL241C	0.718125	0.308207	-0.055246
YDR078C	YDR078C	0.739559	0.334695	-0.081179
YNL093W	YNL093W	0.614381	0.277152	-0.019299
YDR506C	YDR506C	0.625395	0.263215	-0.00256
YDR476C	YDR476C	0.626092	0.247981	0.050717
YFR016C	YFR016C	0.591159	0.266665	0.039515
YER004W	YER004W	0.591986	0.315014	1.49E-04
YDR074W	YDR074W	0.583186	0.350046	0.028166
YAR031W	YAR031W	0.564029	0.188968	0.059759
YHR162W	YHR162W	0.496786	0.193243	-0.050497
YNL103W	YNL103W	0.498302	0.154889	0.012203
YLL056C	YLL056C	0.60499	0.153152	-0.039586
YDL086W	YDL086W	0.564803	0.149282	-0.073255
YPL176C	YPL176C	0.507913	0.266854	-0.086298
YLR454W	YLR454W	0.478648	0.240529	-0.077376
YPL236C	YPL236C	0.484881	0.04149	0.00125
YOR193W	YOR193W	0.425229	0.128259	-0.079949
YKL064W	YKL064W	0.584997	0.279473	0.151076
YOL009C	YOL009C	0.566629	0.266666	0.127476
YBR136W	YBR136W	0.562806	0.260752	0.165813
YHL018W	YHL018W	0.547182	0.345306	0.158555
YKR054C	YKR054C	0.463849	0.292818	0.103726
YNL148C	YNL148C	0.50192	0.302085	0.096515

YHR099W	YHR099W	0.483498	0.281462	0.191462
YKL203C	YKL203C	0.481823	0.420082	0.14131
YGL206C	YGL206C	0.542943	0.371285	0.053108
YFL041W	YFL041W	0.472184	0.363991	0.036445
YKR034W	YKR034W	0.439557	0.262326	0.023869
YCR032W	YCR032W	0.390897	0.374289	0.021102
YGL053W	YGL053W	0.70292	0.15773	-0.309933
YMR196W	YMR196W	0.729957	0.139779	-0.299056
YMR315W	YMR315W	0.581139	0.005065	-0.297006
YER039C	YER039C	0.658019	0.03216	-0.272236
YLR156W	YLR156W	0.687946	-0.006232	-0.209862
YBR006W	YBR006W	0.635928	0.056828	-0.193555
YAL001C	YAL001C	0.550178	0.105731	-0.194594
YPR007C	YPR007C	0.548947	0.082577	-0.257611
YBR076W	YBR076W	0.451802	0.151175	-0.313629
YBL091C-A	YBL091C-A	0.623323	0.231421	-0.24542
YJR008W	YJR008W	0.673995	0.28283	-0.275076
YNL006W	YNL006W	0.658405	0.28475	-0.250896
YHR161C	YHR161C	0.707763	0.227858	-0.135645
YCR091W	YCR091W	0.719086	0.25168	-0.164835
YLR211C	YLR211C	0.716051	0.299954	-0.144395
YIL050W	YIL050W	0.75505	0.244964	-0.217685
YAL062W	YAL062W	0.730282	0.246295	-0.229944
YJL185C	YJL185C	0.639832	0.228435	-0.077771
YPR196W	YPR196W	0.610963	0.242417	-0.143186
YPR079W	YPR079W	0.635556	0.217538	-0.132211
YKR089C	YKR089C	0.680805	0.183049	-0.10222
YPR201W	YPR201W	0.696521	0.190369	-0.160795
YGL250W	YGL250W	0.58896	0.167738	-0.17094
YOR136W	YOR136W	0.59268	0.370343	-0.162238
YDL059C	YDL059C	0.650068	0.330581	-0.139622
YKL193C	YKL193C	0.668065	0.359615	-0.161929
YFR024C-A	YFR024C-A	0.659291	0.333679	-0.219687
YDL223C	YDL223C	0.641747	0.300869	-0.170029
YOR347C	YOR347C	0.681784	0.389476	-0.259869
YKL208W	YKL208W	0.565007	0.422599	-0.257768
YKR013W	YKR013W	0.454937	0.515898	-0.181775
YAR035W	YAR035W	0.613453	0.393402	-0.373743
YBR149W	YBR149W	0.623446	0.281616	-0.367106
YGR244C	YGR244C	0.719554	0.330664	-0.392958
YHR138C	YHR138C	0.633966	0.45974	-0.533666
YOR020W-	YOR020W-	0.651711	0.525487	-0.414666

Table S5: List of Group 2 AA genes

1810 = SWI2 Anchor away; 1854= SWI2 Anchor away sir3 null mutant; 1853 = sir3 null in Anchor away background; 1809 = Wildtype Anchor away background. _R = with Rapamycin

YORF	NAME	1810_R1-1809_R	1854_R1-1809_R	1853_R-1809_R
YFR027W	ECO1	1.066789	-0.045791	-0.669208
YML108W	null	1.029809	-0.137468	-0.538262
YPR148C	null	1.267408	-0.077573	-0.522108
YOL108C	INO4	1.16215	-0.019617	-0.617004
YDL101C	DUN1	1.180908	0.008541	-0.527505
YLR420W	URA4	1.285333	5.47E-04	-0.319895
YOR357C	SNX3	1.25215	0.03339	-0.412955
YDL135C	RDI1	1.203921	-0.001992	-0.216348
YMR263W	SAP30	1.102979	-0.021424	-0.273703
YLR312C-B	null	1.01248	-0.193766	-0.110078
YDR308C	SRB7	1.040916	-0.11343	-0.102671
YNR029C	null	1.050316	-0.128786	-0.059821
YMR029C	FAR8	1.002667	-0.058155	-0.084481
YBR014C	GRX7	1.082561	-0.200944	-0.265018
YCR082W	AHC2	1.088685	-0.130606	-0.218864
YDR130C	FIN1	1.06606	-0.17393	-0.215208
YKL089W	MIF2	1.140109	-0.213645	-0.15261
YFL034C-A	RPL22B	1.033232	-0.217076	-0.193786
YKR035W-	DID2	1.016133	-0.253712	-0.24015
YER030W	CHZ1	1.607177	0.09653	-0.370041
YJR022W	LSM8	1.538216	0.107655	-0.395975
YPR188C	MLC2	1.639887	-0.114558	-0.278256
YOR195W	SLK19	1.516348	-0.219008	-0.286149
YOR194C	TOA1	1.286919	-0.006988	0.012911
YGR135W	PRE9	1.238083	0.063397	-0.014367
YPR100W	MRPL51	1.361305	0.102015	0.122359
YDR315C	IPK1	1.432264	0.036723	0.137238
YPR073C	LTP1	1.425334	0.088795	0.090258
YDR079C-A	TFB5	1.311372	-0.059416	0.088674
YBL090W	MRP21	1.31457	0.003371	0.235119
YIL063C	YRB2	1.424641	0.128045	-0.006819
YDL216C	RRI1	1.484604	0.244172	-0.107044
YKR029C	SET3	1.084159	0.502969	-0.199273
YNL050C	null	1.113443	0.55606	-0.237633
YLR262C	YPT6	1.201175	0.424257	-0.27768
YGL244W	RTF1	1.064341	0.308883	-0.407579
YER170W	ADK2	1.086861	0.311351	-0.253826
YOR094W	ARF3	1.03361	0.259975	-0.280725
YDR162C	NBP2	1.090693	0.510215	-0.584332
YPL045W	VPS16	1.015906	0.632306	-0.45783
YIL138C	TPM2	1.682786	0.306056	-0.690793
YDL161W	ENT1	1.34342	0.389242	-0.723547
YLR148W	PEP3	1.353599	0.187139	-0.569213
YER159C	BUR6	1.670063	0.437402	-0.210862
YEL021W	URA3	1.632845	0.262002	-0.268966

YMR075W	RCO1	1.387632	0.469548	-0.390184
YNL122C	null	1.014566	-0.117233	0.197204
YGL029W	CGR1	1.054287	-0.134631	0.052386
YMR039C	SUB1	1.12259	-0.285114	0.368477
YKR060W	UTP30	1.097246	-0.373862	0.244983
YOR305W	RRG7	1.281278	-0.420408	0.031223
YJL140W	RPB4	1.223792	-0.318465	0.080238
YJR057W	CDC8	1.020569	-0.374342	-0.112441
YBR098W	MMS4	1.162837	0.177413	0.094098
YMR188C	MRPS17	1.092885	0.22016	0.045758
YJL155C	FBP26	1.093268	0.238717	0.093247
YMR158W	MRPS8	1.031525	0.153426	0.08375
YDR004W	RAD57	1.060236	0.106427	0.072368
YKL082C	RRP14	1.108827	0.094592	0.006446
YDR494W	RSM28	1.004573	0.313237	0.0797
YPR131C	NAT3	1.011685	0.308937	-0.040734
YJL162C	JJJ2	1.080659	0.360894	0.010818
YNL084C	END3	1.090977	0.101192	-0.099086
YML015C	TAF11	1.04558	0.105481	-0.175426
YGR029W	ERV1	1.092301	0.227575	-0.105768
YER048C	CAJ1	1.047871	0.271252	-0.17278
YOR266W	PNT1	1.049498	0.285775	-0.183032
YGL230C	null	1.258502	0.156629	-0.213166
YLR051C	FCF2	1.280758	0.207603	-0.12482
YNR032C-A	HUB1	1.214463	0.103032	-0.10574
YCL055W	KAR4	1.211781	0.277987	-0.020767
YDL235C	YPD1	1.260954	0.268571	-0.070049
YJL085W	EXO70	1.179199	0.305385	-0.089646
YDL099W	BUG1	1.234792	0.341265	-0.154571
YMR200W	ROT1	1.204718	0.45217	0.002839
YJL072C	PSF2	1.166446	0.463231	-0.036795
YGL058W	RAD6	1.061177	0.473075	0.046744
YPL108W	null	1.126847	0.43002	0.041395
YGR287C	IMA1	1.13376	0.542336	0.029656
YGL158W	RCK1	1.048703	0.481122	-0.036415
YDL002C	NHP10	1.079376	0.467327	-0.040343
YDR140W	MTQ2	1.088689	0.467984	-0.007828
YGR240C-A	null	1.112271	0.503602	-0.062786
YOL023W	IFM1	1.026897	0.570025	-0.089091
YDR393W	SHE9	1.033013	0.402441	-0.174446
YPR051W	MAK3	1.290515	0.328365	0.088339
YGR196C	FYV8	1.312014	0.364993	0.065092
YBR111W-A	SUS1	1.372997	0.313199	0.013141
YPL052W	OAZ1	1.1649	0.287288	0.032563
YKR014C	YPT52	1.199055	0.350467	0.081193
YNL306W	MRPS18	1.20091	0.284713	0.108797
YPL051W	ARL3	1.289894	0.507288	0.138563
YDR056C	null	1.182859	0.504021	0.170293
YGR215W	RSM27	1.131787	0.178328	0.231714
YKL138C	MRPL31	1.079247	0.208727	0.219332

YGL047W	ALG13	1.157082	0.277432	0.18898
YCR071C	IMG2	1.111693	0.307811	0.281549
YLR312W-	MRPL15	1.190386	0.342826	0.324444
YDR337W	MRPS28	1.09922	0.421759	0.167552
YPR020W	ATP20	1.0745	0.346415	0.162848
YDL119C	null	1.019403	0.384499	0.20403
YLR257W	null	1.103853	0.045546	0.384654
YLR353W	BUD8	1.16627	0.068854	0.30876
YBR035C	PDX3	1.124083	0.174003	0.417988
YLL009C	COX17	1.018919	0.197931	0.401414
YPR072W	NOT5	1.064522	0.078616	0.260964
YKL053C-A	MDM35	1.025934	0.14345	0.201852
YBL038W	MRPL16	1.09796	0.216539	0.324062
YOL133W	HRT1	1.066203	0.142261	0.354629
YGR168C	null	1.028826	0.142986	0.296027
YHR207C	SET5	1.064848	0.256471	0.286648
YOR166C	SWT1	1.018944	0.250358	0.263306
YMR299C	DYN3	1.445678	0.274948	0.279285
YHL022C	SPO11	1.539086	0.169963	0.328393
YDL200C	MGT1	1.517248	0.123993	0.284844
YJL127C-B	null	1.303283	0.155014	0.26686
YDR468C	TLG1	1.333146	0.169745	0.239176
YDR243C	PRP28	1.291768	0.201127	0.195965
YOR148C	SPP2	1.309947	0.185429	0.370267
YMR132C	JLP2	1.343667	0.267558	0.316044
YDR318W	MCM21	1.408467	0.206356	0.359363
YKL137W	CMC1	1.396391	0.152925	0.454729
YDR272W	GLO2	1.406336	0.264159	0.508817
YOL017W	ESC8	1.290712	0.085347	0.530284
YJR082C	EAF6	1.289898	0.193897	0.578618
YKL002W	DID4	1.165457	0.127193	0.593513
YGR153W	null	2.636502	0.65501	-0.717081
YNL056W	OCA2	2.209609	0.202457	0.243769
YCR020W-	HTL1	2.43541	0.626473	0.604439
YLR025W	SNF7	1.549937	0.602071	-0.037162
YML062C	MFT1	1.467596	0.50822	-0.069654
YOR078W	BUD21	1.433841	0.437274	-0.129684
YMR284W	YKU70	1.38401	0.491141	-0.018359
YKL160W	ELF1	1.4777	0.386218	0.03296
YJL013C	MAD3	1.470005	0.373521	0.130819
YDR289C	RTT103	1.539179	0.401045	0.156093
YJR011C	null	1.612044	0.511631	0.185125
YMR197C	VTI1	1.531006	0.565154	0.129688
YDR068W	DOS2	1.553337	0.561149	0.133572
YDR168W	CDC37	1.535247	0.585925	0.192948
YLR170C	APS1	1.752593	0.476661	0.012479
YJL179W	PFD1	1.907616	0.404717	0.135655
YOL086W-	MHF1	2.026676	0.363643	0.046947
YKL138C-A	HSK3	1.988677	0.5422	-0.05758
YDR371W	CTS2	1.884904	0.719605	0.198772

YKL045W	PRI2	1.926462	0.714555	0.301464
YDR357C	CNL1	1.963634	0.278897	0.668585
YBL001C	ECM15	1.897314	0.4213	0.630408
YOR193W	PEX27	1.664403	0.370363	0.792536
YHR018C	ARG4	1.744191	0.212447	0.764307
YBR253W	SRB6	1.66342	0.413677	0.451705
YGL005C	COG7	1.550437	0.465454	0.355049
YOR189W	IES4	1.532081	0.3796	0.363025
YNL032W	SIW14	1.494743	0.417652	0.358942
YLR168C	UPS2	1.598847	0.20454	0.302982
YDR248C	null	1.683574	0.18974	0.364874
YBR258C	SHG1	1.804436	0.157961	0.368224
YDR363W-	SEM1	1.711634	0.394	0.251605
YBL031W	SHE1	1.756326	0.242941	0.215874
YLR298C	YHC1	1.797467	0.789333	0.641127
YFR011C	MIC19	1.778927	0.810115	0.444434
YJR088C	EMC2	1.827402	0.689866	0.51358
YDR163W	CWC15	1.651898	0.668288	0.458456
YOR279C	RFM1	1.514079	0.64749	0.516194
YBR230W-	null	1.661016	0.709246	0.584007
YGL185C	null	1.6241	0.77675	0.646675
YIL161W	null	1.572165	0.753236	0.577457
YEL003W	GIM4	1.548492	0.730687	0.626362
YOR319W	HSH49	1.712134	0.544794	0.677793
YFL059W	SNZ3	1.798037	0.512656	0.610341
YLR040C	AFB1	1.996371	-2.293769	-1.185353
YHR152W	SPO12	1.14144	-0.283468	-0.833568
YNL166C	BNI5	1.037201	-0.219385	-0.741169
YLR200W	YKE2	1.154765	-0.007324	-0.892606
YIL117C	PRM5	1.086923	-0.035356	-0.952209
YKR095W-	PCC1	1.031575	-0.123828	-1.05424
YPR046W	MCM16	1.311028	-0.342763	-1.06318
YBR138C	null	1.670686	0.301455	-1.132607
YFL065C	null	1.158689	0.484584	-1.018472
YBR233W-	DAD3	1.797092	-0.67985	-0.451534
YDR501W	PLM2	1.07483	-0.321768	-0.580323
YAL034W-	MTW1	1.072017	-0.468353	-0.543572
YKL216W	URA1	1.345975	-0.577883	-0.551034
YOL113W	SKM1	1.033519	-0.587046	-0.721315
YIL008W	URM1	1.138537	-0.63178	-0.890334
YNL079C	TPM1	1.001356	-0.43739	-0.914134
YNL129W	NRK1	1.184104	-0.836755	-0.805896
YDR378C	LSM6	1.096922	-0.892641	-0.563517
YFL060C	SNO3	1.033389	-0.973829	-0.694433
YLR154C	RNH203	1.121341	-0.376784	-1.473617
YOR216C	RUD3	1.013053	-0.203636	-1.384204
YNL188W	KAR1	1.113291	-0.931413	-1.394805